

Convergence theory for IETI-DP solvers for discontinuous Galerkin Isogeometric Analysis that is explicit in h and p

Rainer Schneckleitner* and Stefan Takacs†

Abstract

In this paper, we develop a convergence theory for Dual-Primal Isogeometric Tearing and Interconnecting (IETI-DP) solvers for isogeometric multi-patch discretizations of the Poisson problem, where the patches are coupled using discontinuous Galerkin. The presented theory provides condition number bounds that are explicit in the grid sizes h and in the spline degrees p . We give an analysis that holds for various choices for the primal degrees of freedom: vertex values, edge averages, and a combination of both. If only the vertex values or both vertex values and edge averages are taken as primal degrees of freedom, the condition number bound is the same as for the conforming case. If only the edge averages are taken, both the convergence theory and the experiments show that the condition number of the preconditioned system grows with the ratio of the grid sizes on neighboring patches.

1 Introduction

Isogeometric Analysis (IgA), see [17, 8], is an approach for discretizing partial differential equations (PDEs) that has been developed in order to improve the compatibility between computer aided design (CAD) and simulation in comparison to the standard finite element method (FEM). The geometry function, that is used in the CAD system to parameterize the computational domain, is also used for the simulation. These geometry functions are usually spanned by B-splines or non-uniform rational B-splines (NURBS). Following the principle of IgA, we also use such functions for the discretization of the PDE. Since only simple domains can be represented by just one geometry

*schneckleitner@numa.uni-linz.ac.at, Institute of Computational Mathematics, Johannes Kepler University Linz, Austria

†stefan.takacs@ricam.oew.ac.at, Johann Radon Institute Institute for Computational and Applied Mathematics, Austrian Academy of Sciences, Linz, Austria

function (single-patch case), the overall computational domain is usually decomposed into multiple patches, each of which is parameterized using its own geometry function (multi-patch IgA). We focus on non-overlapping patches.

The patches can be coupled either in a conforming way or by means of discontinuous Galerkin methods. For a conforming discretization both the geometry function and the discretization have to agree on the interfaces between the patches. One promising alternative to overcome these restrictions are discontinuous Galerkin approaches, cf. [28, 6], particularly the symmetric interior penalty discontinuous Galerkin (SIPG) method, cf. [5]. The idea of applying this technique to couple patches in IgA, has been previously discussed in [21, 22, 33].

After the discretization of the PDE, we obtain a large-scale linear system and we are interested in fast iterative solvers for such systems. Since we are in a multi-patch framework, domain decomposition solvers are a canonical choice. One of the most popular domain decomposition solvers for large-scale systems of finite element equations in standard FEM is the Finite Element Tearing and Interconnecting method (FETI), originally proposed in [12]. Since the invention of FETI, various FETI-type methods have been developed, cf. [27, 34, 20]. In [19], it was proposed to use a FETI-type method, namely the Dual-Primal FETI method (FETI-DP), in the context of IgA. This method was called Dual-Primal Isogeometric Tearing and Interconnecting (IETI-DP) method. Later, this approach has been further analyzed, particularly in [16] and more recently in [29]. In the latter paper, the authors of the paper at hand have analyzed the dependence of the condition number of the preconditioned system on the spline degree p .

The extension of FETI methods or IETI methods to dG discretizations is not straightforward. We follow the approaches that have been proposed in [11] and adapted for IETI in [14], particularly the idea of using artificial interfaces. Up to the knowledge of the authors, so far, there is no convergence analysis that covers the dependence of the condition number of the preconditioned system on the spline degree p . Moreover, we are not aware of convergence analysis for IETI-DP for dG discretizations that covers the case that only edge averages are taken as primal degrees of freedom. Such approaches might be of interest if the overall computational domain is decomposed into patches in a way that allows T-junctions or in the case of moving patches like in the case of rotating electrical machines.

For conforming finite element discretizations, condition number bounds that are explicit in the polynomial degree p have been worked out previously for FETI-DP type methods, cf. [25, 18], and other Schwarz type, cf. [31, 13], and iterative substructuring methods, cf. [2, 26].

For dG discretizations, there are only a few results concerning a p -analysis for domain decomposition approaches, like [4, 30] for two-level Schwarz type approaches or [10, 7], where the estimates for BDDC and FETI-DP type methods for spectral element methods and hp -FEM are given. The publication [3] shows a bound for general non-

overlapping Schwarz preconditioners for dG hp -FEM that is in the order of p^2 . A polylogarithmic bound for a BDDC preconditioner for a hybridizable discontinuous Galerkin discretization has been developed in [9].

In this paper, we consider the Poisson problem on planar domains. We consider a IETI-DP solver with a scaled Dirichlet preconditioner. The proof follows the abstract framework from [23] and is a continuation of the paper [29], where we have analyzed IETI-DP methods for conforming discretizations. The presented theory covers three different choices for the primal degrees of freedom: vertex values only (Alg. A), edge averages only (Alg. B), and the combination of both (Alg. C). We prove that the condition of the preconditioned IETI-DP solver is bounded by

$$C p \left(1 + \log p + \max_{k=1,\dots,K} \log \frac{H_k}{h_k} \right)^2,$$

for Alg. A and C and by

$$C \delta p \left(\max_{k=1,\dots,K} \max_{\ell \in \mathcal{N}_\Gamma(k)} \frac{h_k}{h_\ell} \right) \left(1 + \log p + \max_{k=1,\dots,K} \log \frac{H_k}{h_k} \right)^2$$

for Alg. B, where p is the spline degree, h_k are the grid sizes and H_k are the patch sizes, $\mathcal{N}_\Gamma(k)$ contains the indices of the patches that share an edge with the k -th patch, and $\delta \geq \delta^*$ is a suitably chosen penalty parameter. Both the constant C and the optimal penalty parameter $\delta^* > 0$ are independent of the grid sizes, the patch sizes, the spline degree and the smoothness of the splines. Hence, the theory covers all discretizations where the smoothness within the patches is between C^0 and C^{p-1} .

The structure of this paper is as follows. In Section 2, we introduce our model problem and its discretization using SIPG. Then, in Section 3, we present the IETI-DP solver. Section 4 is devoted to the proof of the condition number bounds. The numerical results are shown in Section 5. In Section 6, we summarize our findings and give some further remarks.

2 The model problem

We consider the discretization of a homogeneous Poisson problem using multi-patch Isogeometric Analysis, where the coupling between the individual patches is realized using a SIPG approach. Since this paper extends the results of the previous paper [29], which covered conforming discretizations, we aim to use the same notation as in the aforementioned paper. To keep the paper self-contained, we briefly reintroduce the notation.

We consider an open, bounded and simply connected domain $\Omega \subset \mathbb{R}^2$ with Lipschitz boundary $\partial\Omega$. We are interested in solving the homogeneous Poisson problem: find

$u \in H_0^1(\Omega)$ such that

$$\int_{\Omega} \nabla u \cdot \nabla v \, dx = \int_{\Omega} f v \, dx \quad \text{for all } v \in H_0^1(\Omega), \quad (1)$$

where $f \in L_2(\Omega)$ is a given function. Throughout the paper, we denote by $L_2(\Omega)$ and $H^s(\Omega)$, $s \in \mathbb{R}$, the usual Lebesgue and Sobolev spaces, respectively. $H_0^1(\Omega) \subset H^1(\Omega)$ is the subspace of functions whose trace vanishes on $\partial\Omega$. We equip these Hilbert spaces with the usual scalar products $(\cdot, \cdot)_{L_2(\Omega)}$ and $(\cdot, \cdot)_{H^1(\Omega)} := (\nabla \cdot, \nabla \cdot)_{L_2(\Omega)}$, norms $\|\cdot\|_{L_2(\Omega)}$, $\|\cdot\|_{H^s(\Omega)}$, and seminorms $|\cdot|_{H^s(\Omega)}$.

The domain Ω is the composition of K non-overlapping subdomains $\Omega^{(k)}$, i.e.,

$$\overline{\Omega} = \bigcup_{k=1}^K \overline{\Omega^{(k)}} \quad \text{and} \quad \Omega^{(k)} \cap \Omega^{(\ell)} = \emptyset \quad \text{for all } k \neq \ell,$$

where \overline{T} denotes the closure of the set T . We refer to the subdomains $\Omega^{(k)}$ as patches. We assume that every patch $\Omega^{(k)}$ is the image of a geometry function

$$G_k : \widehat{\Omega} := (0, 1)^2 \rightarrow \Omega^{(k)} := G_k(\widehat{\Omega}) \subset \mathbb{R}^2, \quad (2)$$

that can be continuously extended to the closure of $\widehat{\Omega}$. Although the geometry functions can be arbitrary functions, in IgA commonly B-spline or NURBS functions are used. We assume that the geometry function is sufficiently smooth such that the following assumption holds.

Assumption 1. There is a constant $C_1 > 0$ such that

$$\|\nabla G_k\|_{L_\infty(\widehat{\Omega})} \leq C_1 H_k \quad \text{and} \quad \|(\nabla G_k)^{-1}\|_{L_\infty(\widehat{\Omega})} \leq C_1 \frac{1}{H_k}$$

for all $k = 1, \dots, K$, where $H_k > 0$ is the diameter of the patch $\Omega^{(k)}$.

The next assumption guarantees that Ω does not have any T-junctions.

Assumption 2. For any two patch indices $k \neq \ell$, the intersection $\overline{\Omega^{(k)}} \cap \overline{\Omega^{(\ell)}}$ is either a common edge (including the neighboring vertices), a common vertex, or empty.

This assumption also ensures that the pre-images $\widehat{\Gamma}_D^{(k)} := G_k^{-1}(\partial\Omega \cap \partial\Omega^{(k)})$ of the (Dirichlet) boundary $\Gamma_D = \partial\Omega$ consist of whole edges.

For any two neighboring patches $\Omega^{(k)}$ and $\Omega^{(\ell)}$, the common edge is denoted by $\Gamma^{(k,\ell)} = \Gamma^{(\ell,k)}$, and its pre-images by $\widehat{\Gamma}^{(k,\ell)} := G_k^{-1}(\Gamma^{(k,\ell)})$ and $\widehat{\Gamma}^{(\ell,k)} := G_\ell^{-1}(\Gamma^{(\ell,k)})$. We collect the indices of patches sharing an edge in a set:

$$\mathcal{N}_\Gamma(k) := \{\ell \neq k : \Omega^{(k)} \text{ and } \Omega^{(\ell)} \text{ share at least one edge}\}.$$

We do the same for two patches $\Omega^{(k)}$ and $\Omega^{(\ell)}$ sharing only a vertex. We denote that common vertex by $\mathbf{x}^{(k,\ell)} = \mathbf{x}^{(\ell,k)}$, as well as its representations in the parameter domain by $\widehat{\mathbf{x}}^{(k,\ell)} := G_k^{-1}(\mathbf{x}^{(k,\ell)})$ and $\widehat{\mathbf{x}}^{(\ell,k)} := G_\ell^{-1}(\mathbf{x}^{(\ell,k)})$. The indices of the patches that contain a certain corner are collected in the set

$$\mathcal{P}(\mathbf{x}) := \{k : \mathbf{x} \in \overline{\Omega^{(k)}}\}.$$

Moreover, we require that the number of neighbors of a patch is uniformly bounded.

Assumption 3. There is a constant $C_2 > 0$ such that $|\mathcal{P}(\mathbf{x})| \leq C_2$ holds for every corner \mathbf{x} .

After the introduction of the computational domain, we establish the isogeometric function spaces. In IgA, those function spaces are either B-spline or NURBS functions. In this paper, we focus on B-splines. Let $p \in \mathbb{N} := 1, 2, 3, \dots$ be a given spline degree. For ease of notation, we assume that it is the same for all patches. For $n \in \mathbb{N}$, a p -open knot vector

$$\Xi = (\xi_1, \dots, \xi_{n+p+1}) = (\underbrace{\zeta_1, \dots, \zeta_1}_{m_1}, \underbrace{\zeta_2, \dots, \zeta_2}_{m_2}, \dots, \underbrace{\zeta_{N_Z}, \dots, \zeta_{N_Z}}_{m_{N_Z}})$$

with multiplicities $m_1 = m_{N_Z} = p + 1$, and $m_i \in \{1, \dots, p\}$ for $i = 2, \dots, N_Z - 1$ and breakpoints $\zeta_1 < \zeta_2 < \dots < \zeta_{N_Z}$ is the building block for the B-spline basis $(B[p, \Xi, i])_{i=1}^n$. The individual basis functions $B[p, \Xi, i]$ are defined via the Cox-de Boor formula, cf. [8, Eq. (2.1) and (2.2)]. This basis spans the univariate spline space

$$S[p, \Xi] := \text{span}\{B[p, \Xi, 1], \dots, B[p, \Xi, n]\}.$$

Let $\Xi^{(k,1)}$ and $\Xi^{(k,2)}$ be two p -open knot vectors over $(0, 1)$. To get a multivariate spline space $\widehat{V}^{(k)}$ over $\widehat{\Omega}$, we tensorize the two univariate spline spaces. The transformation of $\widehat{V}^{(k)}$ to the physical domain is defined by the pull-back principle. We denote the resulting space by $V^{(k)}$. So, we define

$$\widehat{V}^{(k)} := \{v \in S[p, \Xi^{(k,1)}] \otimes S[p, \Xi^{(k,2)}] : v|_{\widehat{\Gamma}_D^{(k)}} = 0\} \quad \text{and} \quad V^{(k)} := \widehat{V}^{(k)} \circ G_k^{-1}, \quad (3)$$

where $v|_T$ denotes the restriction of v to T (trace operator). The basis for the space $\widehat{V}^{(k)}$ consists of only those tensor-product basis functions over $\Omega^{(k)}$ that vanish on the pre-image of the Dirichlet boundary $\widehat{\Gamma}_D^{(k)}$. Say, the total number of basis functions of $\widehat{V}^{(k)}$ is $N^{(k)} = N_I^{(k)} + N_\Gamma^{(k)}$. The number $N_I^{(k)}$ denotes the number of basis function that are supported only in the interior of the patch whereas $N_\Gamma^{(k)}$ accounts for the number of basis functions that contribute to the boundary of the patch. These definitions give rise to an ordered basis

$$\begin{aligned} \widehat{\Phi}^{(k)} &:= (\widehat{\phi}_i^{(k)})_{i=1}^{N^{(k)}}, \\ \{\widehat{\phi}_i^{(k)}\} &= \{\widehat{\phi} : \exists j_1, j_2 : \widehat{\phi}(x, y) = B[p, \Xi^{(k,1)}, j_1](x) B[p, \Xi^{(k,2)}, j_2](y) \wedge \widehat{\phi}|_{\widehat{\Gamma}_D^{(k)}} = 0\}, \\ \widehat{\phi}_i^{(k)}|_{\partial\widehat{\Omega}} = 0 &\Leftrightarrow i \in \{1, \dots, N_I^{(k)}\}, \quad \text{and} \quad \widehat{\phi}_i^{(k)}|_{\partial\widehat{\Omega}} \neq 0 \Leftrightarrow i \in N_I^{(k)} + \{1, \dots, N_\Gamma^{(k)}\}. \end{aligned} \quad (4)$$

The pull-back principle gives a basis for $V^{(k)}$:

$$\Phi^{(k)} := (\phi_i^{(k)})_{i=1}^{N^{(k)}} \quad \text{and} \quad \hat{\phi}_i^{(k)} := \hat{\phi}_i^{(k)} \circ G_k^{-1}.$$

We assume in the following that the grids on each of the patches are quasi-uniform.

Assumption 4. There are grid sizes $\hat{h}_k > 0$ for $k = 1, \dots, K$ and a constant $C_3 > 0$ such that

$$C_3 \hat{h}_k \leq \zeta_{i+1}^{(k,\delta)} - \zeta_i^{(k,\delta)} \leq \hat{h}_k$$

holds for all $i = 1, \dots, N_Z^{(k,\delta)} - 1$ and all $\delta = 1, 2$.

The corresponding grid size on the physical domain is defined via $h_k := \hat{h}_k H_k$. For any two patches $\Omega^{(k)}$ and $\Omega^{(\ell)}$ sharing an edge, we define

$$\hat{h}_{k\ell} := \min\{\hat{h}_k, \hat{h}_\ell\} \quad \text{and} \quad h_{k\ell} := \min\{h_k, h_\ell\}.$$

The product space of the local spaces $V^{(k)}$ gives the global approximation space

$$V := \prod_{k=1}^K V^{(k)} := V^{(1)} \times \dots \times V^{(K)}. \quad (5)$$

Using these function spaces, the dG discretization of the model problem (1) is given by: find $u = (u^{(1)}, \dots, u^{(K)}) \in V$ such that

$$a_h(u, v) = \langle f, v \rangle \quad \text{for all } v \in V, \quad (6)$$

where

$$\begin{aligned} a_h(u, v) &:= \sum_{k=1}^K (a^{(k)}(u, v) + m^{(k)}(u, v) + r^{(k)}(u, v)), \\ a^{(k)}(u, v) &:= \int_{\Omega^{(k)}} \nabla u^{(k)} \cdot \nabla v^{(k)} \, dx, \\ m^{(k)}(u, v) &:= \sum_{\ell \in \mathcal{N}_\Gamma^{(k)}} \int_{\Gamma^{(k,\ell)}} \frac{1}{2} \left(\frac{\partial u^{(k)}}{\partial n_k} (v^{(\ell)} - v^{(k)}) + \frac{\partial v^{(k)}}{\partial n_k} (u^{(\ell)} - u^{(k)}) \right) \, ds, \\ r^{(k)}(u, v) &:= \sum_{\ell \in \mathcal{N}_\Gamma^{(k)}} \int_{\Gamma^{(k,\ell)}} \frac{\delta p^2}{h_{k\ell}} (u^{(\ell)} - u^{(k)}) (v^{(\ell)} - v^{(k)}) \, ds, \\ \langle f, v \rangle &:= \sum_{k=1}^K \int_{\Omega^{(k)}} f v^{(k)} \, dx, \end{aligned}$$

and $\delta > 0$ is some suitably chosen penalty parameter and n_k is the outward unit normal vector of the patch $\Omega^{(k)}$.

Due to [33, Theorem 8], the parameter δ can always be chosen independently of the spline degree p and mesh sizes h_k such that the bilinear form $a_h(\cdot, \cdot)$ is bounded and coercive in the dG-norm

$$\|v\|_d^2 := d(v, v), \quad \text{where} \quad d(u, v) := \sum_{k=1}^K (a^{(k)}(u, v) + r^{(k)}(u, v)).$$

Note that δ depends on the constant C_1 from Assumption 1. Similar results have been shown previously, but up to the knowledge of the authors, the dependence on p has only been addressed in [33, Theorem 8].

Since we have coercivity and boundedness, the Lax-Milgram lemma ensures the existence of a solution of (6) and its uniqueness. The solution to (6) is an approximation to the solution of the original problem (1), cf. [33, Theorems 12 and 13].

If we choose a basis for V , the discrete variational problem (6) can be rewritten in matrix-vector form. For the setup of a IETI method, we do not need this step since we directly work with the discrete variational problem (6).

3 The dG IETI-DP solver

In this section, we propose a IETI-DP solver for the variational problem (6). As for any tearing and interconnecting method, we have to introduce local spaces, cf., e.g., [12]. As it has been done previously for IETI methods, the local spaces are chosen on a per-patch basis, cf. [19] and later publications on IETI. In the case of dG, the choice is not completely straight-forward. We follow the approach that has been proposed in [11] and that has already been used in an IgA context in [15, 14] and others.

The patch-local subspace consists of the local functions on the particular patch and of those functions from the neighboring patches required to realize the bilinear forms $m^{(k)}(\cdot, \cdot)$ and $r^{(k)}(\cdot, \cdot)$. We define the enriched function space

$$V_e^{(k)} := V^{(k)} \times \prod_{\ell \in \mathcal{N}_\Gamma(k)} V^{(k, \ell)},$$

where $V^{(k, \ell)} := \{v^{(\ell)}|_{\Gamma^{(k, \ell)}} : v^{(\ell)} \in V^{(\ell)}\}$ is the trace of $V^{(\ell)}$. Correspondingly, we write

$$v_e^{(k)} = (v^{(k)}, (v^{(k, \ell)})_{\ell \in \mathcal{N}_\Gamma(k)}) \quad (7)$$

where $v_e^{(k)} \in V_e^{(k)}$, $v^{(k)} \in V^{(k)}$ and $v^{(k, \ell)} \in V^{(k, \ell)}$. Note that the traces of the basis functions

$$\{\phi_1^{(k, \ell)}, \dots, \phi_{N^{(k, \ell)}}^{(k, \ell)}\} := \left\{ \phi_i^{(\ell)}|_{\Gamma^{(k, \ell)}} : \phi_i^{(\ell)} \in \Phi^{(\ell)}, \phi_i^{(\ell)}|_{\Gamma^{(k, \ell)}} \neq 0 \right\}$$

form a basis of $V^{(k, \ell)}$, which is uniquely defined up to the ordering of the basis functions. We denote the basis by $\Phi^{(k, \ell)} := (\phi_i^{(k, \ell)})_{i=1}^{N^{(k, \ell)}}$.

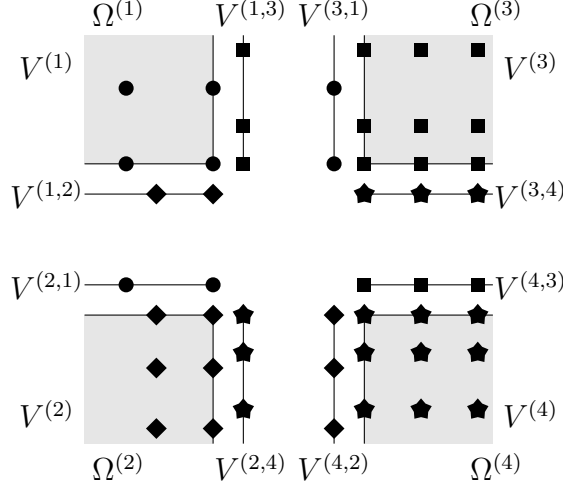


Figure 1: Local spaces with artificial interfaces

This definition can be interpreted as using artificial interfaces. A visualization is given in Fig. 1. The basis functions for each of the patches are represented via different symbols. The location of the symbol is the point where the corresponding basis function takes its maximum. The symbols that are located on the edges and corners represent the only functions that are supported on that edge or corner, respectively. Besides the patches themselves, we have artificial interfaces. While they are co-located with the (standard) interfaces, they are treated as separate entities on which the corresponding trace spaces $V^{(k,\ell)}$ live. The basis functions living on these trace spaces are marked with the same kind of symbol as the basis function from the original space.

Following the structure of (7), we define a basis $\Phi_e^{(k)} := (\phi_{e,i}^{(k)})_{i=1}^{N_e^{(k)}}$ with $N_e^{(k)} := \dim V_e^{(k)}$ for the space $V_e^{(k)}$ as follows. We start with the basis functions from the basis $\Phi^{(k)}$:

$$\phi_{e,i}^{(k)} := (\phi_i^{(k)}, (0, \dots, 0)) \quad \text{for } i = 1, \dots, N^{(k)}.$$

Then, there follow the basis functions from the neighboring patches. Let $\mathcal{N}_\Gamma(k) =$

$\{\ell_1, \ell_2, \dots, \ell_L\}$. We define

$$\begin{aligned}
\phi_{e, \Upsilon_i^{(k, \ell_1)}}^{(k)} &:= (0, (\phi_i^{(k, \ell_1)}, 0 \dots, 0)) \\
&\quad \text{with } \Upsilon_i^{(k, \ell_1)} := N^{(k)} + i && \text{for } i = 1, \dots, N^{(k, \ell_1)}, \\
\phi_{e, \Upsilon_i^{(k, \ell_2)}}^{(k)} &:= (0, (0, \phi_i^{(k, \ell_2)}, 0 \dots, 0)) \\
&\quad \text{with } \Upsilon_i^{(k, \ell_2)} := N^{(k)} + N^{(k, \ell_1)} + i && \text{for } i = 1, \dots, N^{(k, \ell_2)}, \\
&\quad \vdots \\
\phi_{e, \Upsilon_i^{(k, \ell_L)}}^{(k)} &:= (0, (0, \dots, 0, \phi_i^{(k, \ell_L)})) \\
&\quad \text{with } \Upsilon_i^{(k, \ell_L)} := N^{(k)} + N^{(k, \ell_1)} + \dots + N^{(k, \ell_{L-1})} + i && \text{for } i = 1, \dots, N^{(k, \ell_L)}.
\end{aligned} \tag{8}$$

From this construction and from (4), we know that the first $N_I^{(k)}$ basis functions of the basis $\Phi_e^{(k)}$ live in the interior of the patch $\Omega^{(k)}$. The following $N_\Gamma^{(k)}$ basis functions live on the interfaces. Finally, the remaining basis functions live on the artificial interfaces.

On the spaces $V_e^{(k)}$, we define the bilinear forms $a_e^{(k)}(\cdot, \cdot)$ and $d_e^{(k)}(\cdot, \cdot)$ and the linear functional $\langle f_e^{(k)}, \cdot \rangle$ analogous to the global objects $a(\cdot, \cdot)$, $d(\cdot, \cdot)$, and $\langle f, \cdot \rangle$ by

$$\begin{aligned}
a_e^{(k)}(u_e^{(k)}, v_e^{(k)}) &:= a^{(k)}(u_e^{(k)}, v_e^{(k)}) + m^{(k)}(u_e^{(k)}, v_e^{(k)}) + r^{(k)}(u_e^{(k)}, v_e^{(k)}), \\
d_e^{(k)}(u_e^{(k)}, v_e^{(k)}) &:= a^{(k)}(u_e^{(k)}, v_e^{(k)}) + r^{(k)}(u_e^{(k)}, v_e^{(k)}), \\
\langle f_e^{(k)}, v_e^{(k)} \rangle &:= \int_{\Omega^{(k)}} f v^{(k)} dx,
\end{aligned}$$

where we write with a slight abuse of notation

$$\begin{aligned}
a^{(k)}(u_e^{(k)}, v_e^{(k)}) &:= \int_{\Omega^{(k)}} \nabla u^{(k)} \cdot \nabla v^{(k)} dx, \\
m^{(k)}(u_e^{(k)}, v_e^{(k)}) &:= \sum_{\ell \in \mathcal{N}_\Gamma^{(k)}} \int_{\Gamma^{(k, \ell)}} \frac{1}{2} \left(\frac{\partial u^{(k)}}{\partial n_k} (v^{(k, \ell)} - v^{(k)}) + \frac{\partial v^{(k)}}{\partial n_k} (u^{(k, \ell)} - u^{(k)}) \right) ds, \\
r^{(k)}(u_e^{(k)}, v_e^{(k)}) &:= \sum_{\ell \in \mathcal{N}_\Gamma^{(k)}} \int_{\Gamma^{(k, \ell)}} \frac{\delta p^2}{h_{k\ell}} (u^{(k, \ell)} - u^{(k)}) (v^{(k, \ell)} - v^{(k)}) ds.
\end{aligned}$$

The bilinear form $d_e^{(k)}(\cdot, \cdot)$ induces the local dG-norm $\|\cdot\|_{d_e^{(k)}}^2 := d_e^{(k)}(\cdot, \cdot)$, the bilinear form $a_e^{(k)}(\cdot, \cdot)$ the local energy norm $\|\cdot\|_{a_e^{(k)}}^2 := a_e^{(k)}(\cdot, \cdot)$.

By discretizing $a_e^{(k)}(\cdot, \cdot)$ and $\langle f_e^{(k)}, \cdot \rangle$ using the basis $\Phi_e^{(k)}$, we obtain the local system

$$A^{(k)} \underline{u}_e^{(k)} = \underline{f}_e^{(k)}, \tag{9}$$

where $A^{(k)} = [a_e^{(k)}(\phi_{e,j}^{(k)}, \phi_{e,i}^{(k)})]_{i,j=1}^{N_e^{(k)}}$ and $\underline{f}_e^{(k)} = [\langle f_e^{(k)}, \phi_{e,i}^{(k)} \rangle]_{i=1}^{N_e^{(k)}}$. The vector $\underline{u}_e^{(k)} = [u_{e,i}^{(k)}]_{i=1}^{N_e^{(k)}}$ is the coefficient vector representing the function $u_e^{(k)} = \sum_{i=1}^{N_e^{(k)}} u_{e,i}^{(k)} \phi_{e,i}^{(k)}$.

We subdivide the stiffness matrix and the load vector into blocks

$$A^{(k)} = \begin{pmatrix} A_{\text{II}}^{(k)} & A_{\text{I}\Gamma}^{(k)} \\ A_{\Gamma\text{I}}^{(k)} & A_{\Gamma\Gamma}^{(k)} \end{pmatrix} \quad \text{and} \quad \underline{f}_e^{(k)} = \begin{pmatrix} \underline{f}_{\text{I}}^{(k)} \\ \underline{f}_{\Gamma}^{(k)} \end{pmatrix},$$

where the first row and the first column correspond to the first $N_I^{(k)}$ basis functions, i.e., to those supported in the interior of the patch $\Omega^{(k)}$. So, the remainder accounts for both the standard interfaces and the artificial interfaces.

Next, we build the Schur complement system of (9) with respect to the interface degrees of freedom:

$$S^{(k)} \underline{w}_e^{(k)} = \underline{g}_e^{(k)}, \quad (10)$$

where

$$S^{(k)} := A_{\Gamma\Gamma}^{(k)} - A_{\Gamma\text{I}}^{(k)} (A_{\text{II}}^{(k)})^{-1} A_{\text{I}\Gamma}^{(k)} \quad \text{and} \quad \underline{g}_e^{(k)} := \underline{f}_{\Gamma}^{(k)} - A_{\Gamma\text{I}}^{(k)} (A_{\text{II}}^{(k)})^{-1} \underline{f}_{\text{I}}^{(k)}. \quad (11)$$

Once $\underline{w}_e^{(k)}$ has been computed, we get the solution $\underline{u}_e^{(k)}$ of the system (9) by

$$\underline{u}_e^{(k)} = \begin{pmatrix} \underline{u}_{\text{I}}^{(k)} \\ \underline{u}_{\Gamma}^{(k)} \end{pmatrix} = \begin{pmatrix} (A_{\text{II}}^{(k)})^{-1} A_{\text{I}\Gamma}^{(k)} \underline{w}_e^{(k)} \\ \underline{w}_e^{(k)} \end{pmatrix}. \quad (12)$$

The collection of all linear systems (10) for all patches yields a block diagonal linear system

$$S \underline{w} = \underline{g}, \quad (13)$$

where

$$S := \begin{pmatrix} S^{(1)} & & \\ & \ddots & \\ & & S^{(K)} \end{pmatrix}, \quad \underline{w} := \begin{pmatrix} \underline{w}_e^{(1)} \\ \vdots \\ \underline{w}_e^{(K)} \end{pmatrix} \quad \text{and} \quad \underline{g} := \begin{pmatrix} \underline{g}_e^{(1)} \\ \vdots \\ \underline{g}_e^{(K)} \end{pmatrix}.$$

In the following, we introduce the building blocks in order to rewrite the Schur complement system in a variational setting. First, we define function spaces on the skeleton:

$$W := \prod_{k=1}^K W_e^{(k)}, \quad \text{where} \quad W_e^{(k)} := W^{(k)} \times \prod_{\ell \in \mathcal{N}_{\Gamma}^{(k)}} W^{(k,\ell)},$$

$W^{(k)} := \{v|_{\partial\Omega^{(k)}} : v \in V^{(k)}\}$ and $W^{(k,\ell)} := V^{(k,\ell)}$. Analogously to (7), an extended function $w_e^{(k)} \in W_e^{(k)}$ has the form

$$w_e^{(k)} = \left(w^{(k)}, (w^{(k,\ell)})_{\ell \in \mathcal{N}_{\Gamma}^{(k)}} \right),$$

where $w^{(k)} \in W^{(k)}$ and $w^{(k,\ell)} \in W^{(k,\ell)}$. A basis for $W_e^{(k)}$ is given by

$$\check{\Phi}_e^{(k)} := \left(\phi_{e, N_I^{(k)} + i}^{(k)} \right)_{i=1}^{\check{N}_e^{(k)}} \quad \text{with} \quad \check{N}_e^{(k)} := N_e^{(k)} - N_I^{(k)}.$$

As above, the coefficient vector $\underline{w}_e^{(k)} = [w_{e,i}^{(k)}]_{i=1}^{\check{N}_e^{(k)}}$ represents the function

$$w_e^{(k)} = \sum_{i=1}^{\check{N}_e^{(k)}} w_{e,i}^{(k)} \phi_{e, N_I^{(k)}+i}^{(k)} \quad (14)$$

with respect to that basis.

The Schur complements realize the discrete harmonic extension $\mathcal{H}_A^{(k)} : W_e^{(k)} \rightarrow V_e^{(k)}$ with respect to the energy norm $\|\cdot\|_{a_e^{(k)}}$, which is defined as follows. For any $w_e^{(k)} = (w^{(k)}, (w^{(k,\ell)})_{\ell \in \mathcal{N}_\Gamma^{(k)}})$, we have $\mathcal{H}_A^{(k)} w_e^{(k)} = (u^{(k)}, (w^{(k,\ell)})_{\ell \in \mathcal{N}_\Gamma^{(k)}})$, where $u^{(k)}$ is such that

$$\begin{aligned} u^{(k)} &= w^{(k)} \quad \text{on} \quad \partial\Omega^{(k)}, \\ a_e^{(k)} \left((u^{(k)}, (w^{(k,\ell)})_{\ell \in \mathcal{N}_\Gamma^{(k)}}), (v^{(k)}, 0^{|\mathcal{N}_\Gamma^{(k)}|}) \right) &= 0 \quad \text{for all} \quad v^{(k)} \in V_0^{(k)}, \end{aligned} \quad (15)$$

where $V_0^{(k)} := V^{(k)} \cap H_0^1(\Omega^{(k)})$. Note that the standard discrete harmonic extension $\mathcal{H}_h^{(k)} : W^{(k)} \rightarrow V^{(k)}$ is defined by $\mathcal{H}_h^{(k)} w^{(k)} = u^{(k)}$, where $u^{(k)}$ is such that

$$\begin{aligned} u^{(k)} &= w^{(k)} \quad \text{on} \quad \partial\Omega^{(k)}, \\ a^{(k)}(u^{(k)}, v^{(k)}) &= 0 \quad \text{for all} \quad v^{(k)} \in V_0^{(k)}. \end{aligned} \quad (16)$$

In variational form, problem (13) reads as follows: find $w = (w_e^{(1)}, \dots, w_e^{(K)}) \in W$ such that

$$\underbrace{\sum_{k=1}^K a_e^{(k)}(\mathcal{H}_A^{(k)} w_e^{(k)}, \mathcal{H}_A^{(k)} q_e^{(k)})}_{s(w, q) :=} = \underbrace{\sum_{k=1}^K \langle f, \mathcal{H}_A^{(k)} q_e^{(k)} \rangle}_{\langle g, q \rangle :=} \quad \text{for all} \quad q = (q_e^{(1)}, \dots, q_e^{(K)}) \in W.$$

The next step is the introduction of constraints that yield the continuity of the solution. For any two patches $\Omega^{(k)}$ and $\Omega^{(\ell)}$ sharing an edge $\Gamma^{(k,\ell)}$ and any basis function $\phi_i^{(k)}$ supported on that edge, we introduce a constraint

$$w_{e,i^*}^{(k)} - w_{e,j^*}^{(\ell)} = 0 \quad \text{with} \quad i^* = i - N_I^{(k)} \quad \text{and} \quad j^* = \Upsilon_i^{(\ell,k)} - N_I^{(\ell)}, \quad (17)$$

where $\Upsilon_i^{(\ell,k)}$ is as in (8) and $w_{e,i^*}^{(k)}$ and $w_{e,j^*}^{(\ell)}$ are the coefficients of the functions $w_e^{(k)}$ and $w_e^{(\ell)}$. The index shifts by $N_I^{(k)}$ and $N_I^{(\ell)}$ account for the restriction to $W_e^{(k)}$ and $W_e^{(\ell)}$, cf. (14). This constraint ensures that the function values of the solution on the artificial interfaces coincide with the function values of the solution on the corresponding standard interfaces.

If the corner values are chosen as primal degrees of freedom (Alg. A and C), we omit the constraints for the basis functions $\phi_i^{(k)}$ that are supported on a corner of $\Omega^{(k)}$. A visualization of the constraints is given in Figure 2.

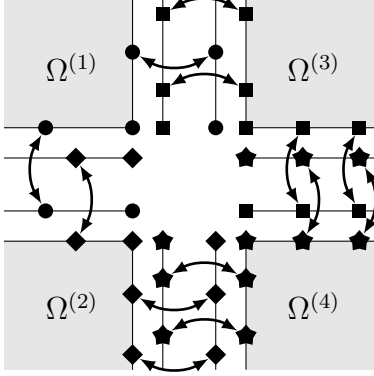


Figure 2: Omitting vertices (Alg. A and C)

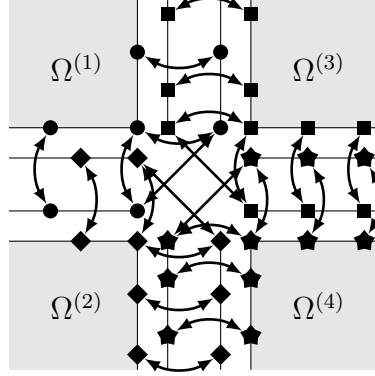


Figure 3: Fully redundant (Alg. B)

If only the edge averages are chosen as primal degrees of freedom (Alg. B), we realize the constraints at the corners in a fully redundant way. This means that besides the constraints (17), for every basis function $\phi_i^{(k)}$ that is supported on a corner of $\Omega^{(k)}$, we additionally introduce constraints of the form

$$w_{e,j_1^*}^{(\ell_1)} - w_{e,j_2^*}^{(\ell_2)} = 0 \quad \text{with} \quad j_1^* = \Upsilon_i^{(\ell_1,k)} - N_I^{(\ell_1)} \quad \text{and} \quad j_2^* = \Upsilon_i^{(\ell_2,k)} - N_I^{(\ell_2)} \quad (18)$$

where $\ell_1 < \ell_2$ such that the said corner lies between the edges $\Gamma^{(k,\ell_1)}$ and $\Gamma^{(k,\ell_2)}$. These additional constraints also ensure the continuity between the different artificial interfaces. A visualization of this case is given in Figure 3.

We collect the constraints of the form (17) and (18) in a matrix B such that the constraints are equivalent to

$$B \underline{w} = 0.$$

This is done such that each row of the matrix corresponds to one constraint, i.e., each row has only two non-zero entries, one with value 1 and one with value -1 . The matrix B can also be represented with patch-local contributions $B^{(1)}, \dots, B^{(K)}$ as $B = (B^{(1)} \dots B^{(K)})$.

We are now able to write down a saddle point problem in matrix-vector form that is equivalent to problem (6): find $(\underline{w}, \underline{\lambda})$ such that

$$\begin{pmatrix} S & B^\top \\ B & \end{pmatrix} \begin{pmatrix} \underline{w} \\ \underline{\lambda} \end{pmatrix} = \begin{pmatrix} \underline{g} \\ 0 \end{pmatrix}.$$

Note that the matrices $A^{(k)}$ and $S^{(k)}$ are non-singular only if the corresponding patch contributes to the Dirichlet boundary $\partial\Omega$. Since in general at least one of the matrices $S^{(k)}$ is singular, the matrix S is usually singular.

The remedy for this problem are primal degrees of freedom which form a global but small linear system. As mentioned in the introduction, we consider three options: Alg. A, B, and C. Each of them corresponds to a different choice of spaces \widetilde{W} and \widetilde{W}_Δ .

- *Alg. A (Vertex values)*: The space \widetilde{W} is the subspace of functions where the vertex values agree, i.e.,

$$\widetilde{W} := \left\{ w \in W : \begin{array}{l} w^{(k)}(\mathbf{x}) = w^{(\ell,k)}(\mathbf{x}) \\ \text{for all common vertices } \mathbf{x} \text{ of all } \Omega^{(k)} \text{ and all } \Omega^{(\ell)} \end{array} \right\}.$$

The space \widetilde{W}_Δ satisfies these conditions homogeneously, i.e., $\widetilde{W}_\Delta := \prod_{k=1}^K \widetilde{W}_\Delta^{(k)}$ and

$$\widetilde{W}_\Delta^{(k)} := \left\{ w_e^{(k)} \in W_e^{(k)} : \begin{array}{l} w^{(k)}(\mathbf{x}) = w^{(\ell,k)}(\mathbf{x}) = 0 \\ \text{for all common vertices } \mathbf{x} \text{ of } \Omega^{(k)} \text{ and all } \Omega^{(\ell)} \end{array} \right\}.$$

- *Alg. B (Edge averages)*: The space \widetilde{W} is the subspace of functions where the averages of the function values over the edges agree, i.e.,

$$\widetilde{W} := \left\{ w \in W : \int_{\Gamma^{(k,\ell)}} w^{(k)}(x) dx = \int_{\Gamma^{(k,\ell)}} w^{(\ell,k)}(x) dx \text{ for all edges } \Gamma^{(k,\ell)} \right\}.$$

The space \widetilde{W}_Δ satisfies these conditions homogeneously, i.e., $\widetilde{W}_\Delta := \prod_{k=1}^K \widetilde{W}_\Delta^{(k)}$ and

$$\widetilde{W}_\Delta^{(k)} := \left\{ w_e^{(k)} \in W_e^{(k)} : \int_{\Gamma^{(k,\ell)}} w^{(k)}(x) dx = \int_{\Gamma^{(k,\ell)}} w^{(k,\ell)}(x) dx = 0 \text{ for all } \Gamma^{(k,\ell)} \right\}.$$

- *Alg. C (Vertex values and edge averages)*: We combine the constraints from both cases. So, the spaces \widetilde{W} and $\widetilde{W}_\Delta^{(k)}$ and \widetilde{W}_Δ are the intersections of the corresponding spaces obtained by Alg. A and B.

The primal space \widetilde{W}_Π is the subspace of energy minimizing functions, cf. [27]. This means that \widetilde{W}_Π is S -orthogonal to \widetilde{W}_Δ , i.e.,

$$\widetilde{W}_\Pi := \{ w \in \widetilde{W} : s(w, q) = 0 \text{ for all } q \in \widetilde{W}_\Delta \}. \quad (19)$$

Let $\psi^{(1)}, \dots, \psi^{(N_\Pi)}$ be a basis of \widetilde{W}_Π . In practice, one usually chooses a nodal basis, where the vertex values and/or the edge averages form the nodal values. The matrix Ψ represents the basis in terms of the basis for the space W , i.e.,

$$\Psi = \begin{pmatrix} \underline{\psi}^{(1)} \\ \vdots \\ \underline{\psi}^{(N_\Pi)} \end{pmatrix}. \quad (20)$$

A representation for the spaces $\widetilde{W}_\Delta^{(k)}$ can be obtained by full-rank matrices $C^{(k)}$:

$$C^{(k)} \underline{w}_e^{(k)} = 0 \quad \Leftrightarrow \quad w_e^{(k)} \in \widetilde{W}_\Delta^{(k)}.$$

The block-diagonal collection of the matrices $C^{(k)}$ gives the matrix

$$C := \begin{pmatrix} C^{(1)} & & \\ & \ddots & \\ & & C^{(K)} \end{pmatrix}.$$

As in [23], the following problem is an equivalent reformulation of (6): find $(\underline{w}_\Delta, \underline{\mu}, \underline{w}_\Pi, \underline{\lambda})$ such that

$$\begin{pmatrix} S & C^\top & & B^\top \\ C & & & \\ & \Psi^\top S \Psi & \Psi^\top B^\top & \\ B & B \Psi & & \end{pmatrix} \begin{pmatrix} \underline{w}_\Delta \\ \underline{\mu} \\ \underline{w}_\Pi \\ \underline{\lambda} \end{pmatrix} = \begin{pmatrix} \underline{g} \\ 0 \\ \Psi^\top \underline{g} \\ 0 \end{pmatrix}.$$

The solution for the original problem is obtained by $\underline{w} = \underline{w}_\Delta + \Psi \underline{w}_\Pi$. Following the DP approach, this system can be reduced to the subsequent problem for the Lagrange multipliers $\underline{\lambda}$:

$$F \underline{\lambda} = \underline{d}, \quad (21)$$

where

$$F := \underbrace{\begin{pmatrix} B & 0 & B \Psi \end{pmatrix} \begin{pmatrix} S & C^\top \\ C & \Psi^\top S \Psi \end{pmatrix}^{-1} \begin{pmatrix} I \\ 0 \\ \Psi^\top \end{pmatrix}}_{F_0 :=} B^\top \quad \text{and} \quad \underline{d} := F_0 \underline{g}. \quad (22)$$

The system (21) is solved with a preconditioned conjugate gradient (PCG) solver. In order to obtain an effective solver, we need a proper preconditioner. We use the scaled Dirichlet preconditioner M_{sD} , defined by

$$M_{\text{sD}} := B D^{-1} S D^{-1} B^\top,$$

where $D \in \mathbb{R}^{N_\Gamma \times N_\Gamma}$ is a diagonal matrix defined based on the principle of multiplicity scaling: Each coefficient $d_{i,i}$ of D is assigned the number of constraints for the corresponding degree of freedom plus one i.e.,

$$d_{i,i} := 1 + \sum_{j=1}^{N_\Gamma} b_{j,i}^2,$$

where $b_{i,j}$ are the coefficients of the matrix B .

The dG IETI-DP method requires the execution of the following steps.

- Compute the right-hand sides $\underline{g}_e^{(k)}$ according to (11).
- Compute the basis Ψ for the primal space in accordance with (19) and (20).

- Compute the primal Schur complement $S_{\Pi} := \Psi^{\top} S \Psi$.
- Solve (21) for $\underline{\lambda}$ using a PCG solver. This requires the computation of the residual and the application of the preconditioner.

The computation of the residual $\widehat{w} := F \underline{\lambda} - \underline{d}$ requires the following steps:

1. Compute $\widehat{q} = ((\widehat{q}_e^{(1)})^{\top} \cdots (\widehat{q}_e^{(K)})^{\top})^{\top} := B^{\top} \underline{\lambda} - \underline{g}$.
2. Solve the linear system

$$\begin{pmatrix} S^{(k)} & (C^{(k)})^{\top} \\ C^{(k)} & \end{pmatrix} \begin{pmatrix} \widehat{w}_{\Delta}^{(k)} \\ \widehat{\mu}^{(k)} \end{pmatrix} = \begin{pmatrix} \widehat{q}_e^{(k)} \\ 0 \end{pmatrix} \quad (23)$$

for all $k = 1, \dots, K$. For Alg. A and C, one usually reduces the local systems by eliminating the degrees of freedom corresponding to the vertex values and the corresponding Lagrange multipliers.

3. Solve the (usually small) global linear system

$$S_{\Pi} \widehat{w}_{\Pi} = \Psi^{\top} \widehat{q}. \quad (24)$$

4. Compute the residual

$$\widehat{w} := B \begin{pmatrix} \widehat{w}_{\Delta}^{(1)} \\ \vdots \\ \widehat{w}_{\Delta}^{(K)} \end{pmatrix} + B \Psi \widehat{w}_{\Pi}. \quad (25)$$

The application of the preconditioner to the residual, i.e., the computation of $M_{\text{sD}} \widehat{w}$, only requires matrix-vector multiplications.

- The vector \underline{w} , representing the solution on the skeleton, is computed analogously to (23), (24) and (25) based on $q = ((q^{(1)})^{\top}) \cdots (q^{(K)})^{\top})^{\top} := B^{\top} \underline{\lambda}$. Finally, the solution vector \underline{u} is derived by (12).

4 The condition number estimate

In this section, we prove the following condition number estimates.

Theorem 4.1. *Provided that the IETI-DP solver is set up as outlined in the previous sections, the condition number of the preconditioned system satisfies*

$$\kappa(M_{\text{sD}} F) \leq C p \left(1 + \log p + \max_{k=1, \dots, K} \log \frac{H_k}{h_k} \right)^2$$

for Alg. A and C and

$$\kappa(M_{\text{sD}}F) \leq C \delta p \left(\max_{k=1,\dots,K} \max_{\ell \in \mathcal{N}_\Gamma(k)} \frac{h_k}{h_\ell} \right) \left(1 + \log p + \max_{k=1,\dots,K} \log \frac{H_k}{h_k} \right)^2$$

for Alg. B, where in both cases the constant C only depends on the constants from the Assumptions 1, 3, and 4.

If some Lagrange multipliers are redundant to each other or to primal constraints, the matrices M_{sD} and F are singular. Standard iteration schemes live in the corresponding factor space. Here and in what follows, the condition number is estimated for the restriction to the factor space, cf. [23, Remark 23].

Notation. We use the notation $a \lesssim b$ if there is a constant $c > 0$ that only depends on the constants from the Assumptions 1, 3, and 4 such that $a \leq cb$. Moreover, we write $a \approx b$ if $a \lesssim b \lesssim a$.

When it is clear from the context, we do not denote the restriction of a function to an interface explicitly, so we write for example $\|u^{(k)}\|_{L_2(\Gamma^{(k,\ell)})}$ instead of $\|u^{(k)}|_{\Gamma^{(k,\ell)}}\|_{L_2(\Gamma^{(k,\ell)})}$.

Before we dive into the condition number estimate, we observe that the bilinear forms $a_e^{(k)}(\cdot, \cdot)$ and $d_e^{(k)}(\cdot, \cdot)$ are patchwise equivalent.

Lemma 4.2. *For every patch $\Omega^{(k)}$,*

$$a_e^{(k)}(u_e^{(k)}, u_e^{(k)}) \lesssim d_e^{(k)}(u_e^{(k)}, u_e^{(k)}) \lesssim a_e^{(k)}(u_e^{(k)}, u_e^{(k)})$$

holds for all $u_e^{(k)} \in V_e^{(k)}$.

Proof. Completely analogous to the proof of [33, Theorem 8]. \square

Analogous to [29, Lemma 4.16], the following lemma allows to estimate the action of the matrix $B_D^\top B$.

Lemma 4.3. *Let $u = (u_e^{(1)}, \dots, u_e^{(K)}) = ((u^{(1)}, (u^{(1,\ell)})_{\ell \in \mathcal{N}_\Gamma(1)}, \dots) \in \widetilde{W}$ with coefficient vector \underline{u} and let $w = (w_e^{(1)}, \dots, w_e^{(K)}) = ((w^{(1)}, (w^{(1,\ell)})_{\ell \in \mathcal{N}_\Gamma(1)}, \dots) \in \widetilde{W}$ with coefficient vector \underline{w} be such that $\underline{w} = B_D^\top B \underline{u}$. Then, we have for each patch $\Omega^{(k)}$ and each edge $\Gamma^{(k,\ell)}$ connecting the vertices $\mathbf{x}^{(k,\ell,1)}$ and $\mathbf{x}^{(k,\ell,2)}$*

$$\begin{aligned} & \|w^{(k)} - w^{(k,\ell)}\|_{L_2(\Gamma^{(k,\ell)})}^2 \\ & \lesssim \|u^{(k)} - u^{(k,\ell)}\|_{L_2(\Gamma^{(k,\ell)})}^2 + \|u^{(\ell)} - u^{(\ell,k)}\|_{L_2(\Gamma^{(k,\ell)})}^2 + \sum_{i=1}^2 \left(\frac{h_k}{p} \Delta^{(k,\ell,i)} + \frac{h_\ell}{p} \Delta^{(\ell,k,i)} \right), \\ & |w^{(k)}|_{H^{1/2}(\Gamma^{(k,\ell)})}^2 \lesssim |u^{(k)}|_{H^{1/2}(\Gamma^{(k,\ell)})}^2 + |u^{(\ell,k)}|_{H^{1/2}(\Gamma^{(k,\ell)})}^2 + \sum_{i=1}^2 \Delta^{(k,\ell,i)}, \end{aligned}$$

and

$$|w^{(k)}|_{L_\infty^0(\Gamma^{(k,\ell)})}^2 \lesssim |u^{(k)}|_{L_\infty^0(\Gamma^{(k,\ell)})}^2 + |u^{(\ell,k)}|_{L_\infty^0(\Gamma^{(k,\ell)})}^2 + \sum_{i=1}^2 \Delta^{(k,\ell,i)},$$

where

$$\Delta^{(k,\ell,i)} := \begin{cases} 0 & \text{for Alg. A and C} \\ \sum_{j \in \mathcal{P}(\mathbf{x}^{(k,\ell,i)}) \cap \mathcal{N}_{\Gamma^{(k)}}} |u^{(k)}(\mathbf{x}^{(k,\ell,i)}) - u^{(j,k)}(\mathbf{x}^{(k,\ell,i)})|^2 & \text{for Alg. B.} \end{cases} \quad (26)$$

Proof. We start by recalling how the scaling matrix D looks like. Remember D is a diagonal matrix. We denote the coefficients by $d_{i,i}$ for $i = 1, \dots, N_\Gamma$. The entries $d_{i,i}$ are defined to be one plus the number of Lagrange multipliers of the corresponding degree of freedom i . Note that we have $d_{i,i} = 2$ unless the corresponding degree of freedom is a corner degree of freedom. In that case, $d_{i,i}$ takes a value, which is bounded from below by 1 and bounded from above due to Assumption 3. Thus, $d_{i,i} \approx 1$ in any case.

We will start with Alg. A and C: Simple calculations reveal for Alg. A and C that

$$\begin{aligned} w^{(k)}|_{\Gamma^{(k,\ell)}} &= \frac{1}{2} \left(u^{(k)}|_{\Gamma^{(k,\ell)}} - u^{(\ell,k)} - \sum_{i=1}^2 \theta^{(k,\ell,i)} (u^{(k)}(\mathbf{x}^{(k,\ell,i)}) - u^{(\ell,k)}(\mathbf{x}^{(k,\ell,i)})) \right), \\ w^{(k,\ell)} &= \frac{1}{2} \left(u^{(k,\ell)} - u^{(\ell)}|_{\Gamma^{(k,\ell)}} - \sum_{i=1}^2 \theta^{(\ell,k,i)} (u^{(k,\ell)}(\mathbf{x}^{(k,\ell,i)}) - u^{(\ell)}(\mathbf{x}^{(k,\ell,i)})) \right). \end{aligned}$$

where $\theta^{(k,\ell,i)}$ is the basis function in $\Phi^{(k)}$ such that $\theta^{(k,\ell,i)}(\mathbf{x}^{(k,\ell,i)}) = 1$. $\theta^{(\ell,k,i)}$ is defined analogously. Since u satisfies the primal constraints, we have $u^{(k)}(\mathbf{x}^{(k,\ell,i)}) = u^{(\ell,k)}(\mathbf{x}^{(k,\ell,i)})$ and $u^{(k,\ell)}(\mathbf{x}^{(k,\ell,i)}) = u^{(\ell)}(\mathbf{x}^{(k,\ell,i)})$ and thus

$$w^{(k)}|_{\Gamma^{(k,\ell)}} = \frac{1}{2} (u^{(k)}|_{\Gamma^{(k,\ell)}} - u^{(\ell,k)}), \quad w^{(k,\ell)} = \frac{1}{2} (u^{(k,\ell)} - u^{(\ell)}|_{\Gamma^{(k,\ell)}}).$$

Therefore, we obtain by using the triangle inequality

$$\|w^{(k)} - w^{(k,\ell)}\|_{L_2(\Gamma^{(k,\ell)})}^2 \lesssim \|u^{(k)} - u^{(k,\ell)}\|_{L_2(\Gamma^{(k,\ell)})}^2 + \|u^{(\ell)} - u^{(\ell,k)}\|_{L_2(\Gamma^{(k,\ell)})}^2$$

for the L_2 -norm. For the $H^{1/2}$ -seminorm, we get using the triangle inequality that

$$|w^{(k)}|_{H^{1/2}(\Gamma^{(k,\ell)})}^2 \lesssim |u^{(k)}|_{H^{1/2}(\Gamma^{(k,\ell)})}^2 + |u^{(\ell,k)}|_{H^{1/2}(\Gamma^{(k,\ell)})}^2.$$

Analogously, we obtain using the triangle inequality

$$|w^{(k)}|_{L_\infty^0(\Gamma^{(k,\ell)})}^2 \lesssim |u^{(k)}|_{L_\infty^0(\Gamma^{(k,\ell)})}^2 + |u^{(\ell,k)}|_{L_\infty^0(\Gamma^{(k,\ell)})}^2,$$

which finishes the proof for the Alg. A and C.

For Alg. B we have that $w^{(k)}$ on $\Gamma^{(k,\ell)}$ can be expanded as

$$\begin{aligned} w^{(k)}|_{\Gamma^{(k,\ell)}} &= \frac{1}{2} \left(u^{(k)}|_{\Gamma^{(k,\ell)}} - u^{(\ell,k)} - \sum_{i=1}^2 \theta^{(k,\ell,i)} (u^{(k)}(\mathbf{x}^{(k,\ell,i)}) - u^{(\ell,k)}(\mathbf{x}^{(k,\ell,i)})) \right) \\ &\quad + \sum_{i=1}^2 \frac{1}{d_{n_i, n_i}} \theta^{(k,\ell,i)} \sum_{j \in \mathcal{P}(\mathbf{x}^{(k,\ell,i)}) \cap \mathcal{N}_{\Gamma}(k)} (u^{(k)}(\mathbf{x}^{(k,\ell,i)}) - u^{(j,k)}(\mathbf{x}^{(k,\ell,i)})), \\ w^{(k,\ell)} &= \frac{1}{2} \left(u^{(k,\ell)} - u^{(\ell)}|_{\Gamma^{(k,\ell)}} - \sum_{i=1}^2 \theta^{(\ell,k,i)} (u^{(k,\ell)}(\mathbf{x}^{(k,\ell,i)}) - u^{(\ell)}(\mathbf{x}^{(k,\ell,i)})) \right) \\ &\quad + \sum_{i=1}^2 \frac{1}{d_{m_i, m_i}} \theta^{(\ell,k,i)} \sum_{j \in (\mathcal{P}(\mathbf{x}^{(k,\ell,i)}) \cap \mathcal{N}_{\Gamma}(\ell)) \cup \{\ell\}} (u^{(k,\ell)}(\mathbf{x}^{(k,\ell,i)}) - u^{(j,\ell)}(\mathbf{x}^{(k,\ell,i)})), \end{aligned}$$

where d_{n_i, n_i} and d_{m_i, m_i} denote the entries of the matrix D for the corresponding dofs and we use $u^{(\ell,\ell)} := u^{(\ell)}$. Note that $\theta^{(k,\ell,i)}$ behaves like $\max\{0, 1 - |x - \mathbf{x}^{(k,\ell,i)}|/h^{(k)}\}^p$. Hence,

$$\begin{aligned} \|\theta^{(k,\ell,i)}\|_{L_2(\Gamma^{(k,\ell)})}^2 &\approx \frac{h_k}{p}, \\ |\theta^{(k,\ell,i)}|_{H^{1/2}(\Gamma^{(k,\ell)})}^2 &\leq |\theta^{(k,\ell,i)}|_{H^1(\Gamma^{(k,\ell)})} \|\theta^{(k,\ell,i)}\|_{L_2(\Gamma^{(k,\ell)})} \approx 1, \text{ and} \\ \|\theta^{(k,\ell,i)}\|_{L_\infty(\Gamma^{(k,\ell)})}^2 &= 1. \end{aligned}$$

An application of the triangle inequality for the corner expressions yields the stated result for Alg. B. \square

The following lemma allows to estimate the $H^{1/2}$ -seminorm on the artificial edges.

Lemma 4.4. *For any two patches $\Omega^{(k)}$ and $\Omega^{(\ell)}$ that share an edge $\Gamma^{(k,\ell)}$, the estimate*

$$|u^{(k,\ell)}|_{H^{1/2}(\Gamma^{(k,\ell)})}^2 \lesssim |u^{(k)}|_{H^{1/2}(\Gamma^{(k,\ell)})}^2 + \frac{p^2}{h_{k\ell}} \|u^{(k,\ell)} - u^{(k)}\|_{L_2(\Gamma^{(k,\ell)})}^2$$

holds for all $u_e^{(k)} = (u^{(k)}, (u^{(k,\ell)})_{\ell \in \mathcal{N}_{\Gamma}(k)}) \in V_e^{(k)}$.

Proof. Let $c \in \mathbb{R}$ be arbitrary but fixed. Using the triangle inequality, we have

$$\|u^{(k,\ell)} - c\|_{H^{1/2}(\Gamma^{(k,\ell)})}^2 \lesssim \|u^{(k)} - c\|_{H^{1/2}(\Gamma^{(k,\ell)})}^2 + \|(u^{(k)} - c) - (u^{(k,\ell)} - c)\|_{H^{1/2}(\Gamma^{(k,\ell)})}^2.$$

Using [1, Theorem 5.2, eq. (3)] and the triangle inequality, we obtain further

$$\begin{aligned} &\|u^{(k,\ell)} - c\|_{H^{1/2}(\Gamma^{(k,\ell)})}^2 \\ &\lesssim \|u^{(k)} - c\|_{H^{1/2}(\Gamma^{(k,\ell)})}^2 + \|u^{(k)} - u^{(k,\ell)}\|_{L_2(\Gamma^{(k,\ell)})} \|(u^{(k)} - c) - (u^{(k,\ell)} - c)\|_{H^1(\Gamma^{(k,\ell)})} \\ &\leq \|u^{(k)} - c\|_{H^{1/2}(\Gamma^{(k,\ell)})}^2 \\ &\quad + \|u^{(k)} - u^{(k,\ell)}\|_{L_2(\Gamma^{(k,\ell)})} (\|u^{(k)} - c\|_{H^1(\Gamma^{(k,\ell)})} + \|u^{(k,\ell)} - c\|_{H^1(\Gamma^{(k,\ell)})}). \end{aligned}$$

Using the equivalence of the norms on the parameter domain and the physical domain, cf. [29, Lemma 4.13], and an inverse inequality, cf. [32, Lemma 4.3] and using $h_{k\ell} = \min\{h_k, h_\ell\}$, we obtain further

$$\begin{aligned} \|u^{(k,\ell)} - c\|_{H^{1/2}(\Gamma^{(k,\ell)})}^2 &\leq \|u^{(k)} - c\|_{H^{1/2}(\Gamma^{(k,\ell)})}^2 \\ &\quad + \frac{C p}{h_{k\ell}^{1/2}} \|u^{(k)} - u^{(k,\ell)}\|_{L_2(\Gamma^{(k,\ell)})} \left(\|u^{(k)} - c\|_{H^{1/2}(\Gamma^{(k,\ell)})} + \|u^{(k,\ell)} - c\|_{H^{1/2}(\Gamma^{(k,\ell)})} \right), \end{aligned}$$

where $C > 0$ is an appropriately chosen constant (that only depends on the constant from Assumption 1). Using $ab \leq a^2 + b^2/4$ and using $(a + b)^2 \leq 2(a^2 + b^2)$, we have

$$\begin{aligned} &\|u^{(k,\ell)} - c\|_{H^{1/2}(\Gamma^{(k,\ell)})}^2 \\ &\leq \|u^{(k)} - c\|_{H^{1/2}(\Gamma^{(k,\ell)})}^2 + \frac{C^2 p^2}{h_{k\ell}} \|u^{(k)} - u^{(k,\ell)}\|_{L_2(\Gamma^{(k,\ell)})}^2 \\ &\quad + \frac{1}{4} \left(\|u^{(k)} - c\|_{H^{1/2}(\Gamma^{(k,\ell)})} + \|u^{(k,\ell)} - c\|_{H^{1/2}(\Gamma^{(k,\ell)})} \right)^2 \\ &\leq \frac{3}{2} \|u^{(k)} - c\|_{H^{1/2}(\Gamma^{(k,\ell)})}^2 + \frac{C^2 p^2}{h_{k\ell}} \|u^{(k)} - u^{(k,\ell)}\|_{L_2(\Gamma^{(k,\ell)})}^2 + \frac{1}{2} \|u^{(k,\ell)} - c\|_{H^{1/2}(\Gamma^{(k,\ell)})}^2. \end{aligned}$$

By subtracting $\frac{1}{2} \|u^{(k,\ell)} - c\|_{H^{1/2}(\Gamma^{(k,\ell)})}^2$, we immediately obtain

$$|u^{(k,\ell)}|_{H^{1/2}(\Gamma^{(k,\ell)})}^2 \leq \|u^{(k,\ell)} - c\|_{H^{1/2}(\Gamma^{(k,\ell)})}^2 \lesssim \|u^{(k)} - c\|_{H^{1/2}(\Gamma^{(k,\ell)})}^2 + \frac{p^2}{h_{k\ell}} \|u^{(k)} - u^{(k,\ell)}\|_{L_2(\Gamma^{(k,\ell)})}^2$$

for all $u_e^{(k)} \in V_e^{(k)}$. Since this holds for all $c \in \mathbb{R}$, the Poincaré inequality yields the desired result. \square

The next step is to show that a similar estimate holds for the seminorm

$$|v|_{L_\infty^0(T)} := \inf_{c \in \mathbb{R}} \|v - c\|_{L_\infty(T)}.$$

Before we can prove that result, we need the following auxiliary result.

Lemma 4.5. *The estimate*

$$\|u\|_{L_\infty(0,1)}^2 \leq \sqrt{2} \|u\|_{L_2(0,1)} \|u\|_{H^1(0,1)}$$

holds for all $u \in H^1(0,1)$.

Proof. Since u is continuous, u takes its maximum for some $z \in [0,1]$. Then, by the fundamental theorem of differential and integral calculus we can write

$$|u(z)|^2 = - \int_z^t u(s)u'(s) \, ds + |u(t)|^2.$$

Next, we integrate over the unit interval and use the Cauchy-Schwarz inequality to obtain

$$\begin{aligned} |u(z)|^2 &= - \int_0^1 \int_z^t u(s)u'(s) ds + |u(t)|^2 dt \leq \int_0^1 \|u\|_{L_2(z,t)} \|u'\|_{L_2(z,t)} dt + \int_0^1 |u(t)|^2 dt \\ &\leq \int_0^1 \|u\|_{L_2(0,1)} \|u'\|_{L_2(0,1)} dt + \|u\|_{L_2(0,1)}^2 = \|u\|_{L_2(0,1)} (\|u'\|_{L_2(0,1)} + \|u\|_{L_2(0,1)}) \\ &\leq \sqrt{2} \|u\|_{L_2(0,1)} \|u\|_{H^1(0,1)}, \end{aligned}$$

which was to show. \square

The next lemma allows to estimate the L_∞^0 -seminorm similar to Lemma 4.4.

Lemma 4.6. *For any two patches $\Omega^{(k)}$ and $\Omega^{(\ell)}$ that share an edge $\Gamma^{(k,\ell)}$, the inequality*

$$|u^{(k,\ell)}|_{L_\infty^0(\Gamma^{(k,\ell)})}^2 \lesssim |u^{(k)}|_{L_\infty^0(\Gamma^{(k,\ell)})}^2 + |u^{(k)}|_{H^{1/2}(\Gamma^{(k,\ell)})}^2 + \frac{p^2}{h_{k\ell}} \|u^{(k)} - u^{(k,\ell)}\|_{L_2(\Gamma^{(k,\ell)})}^2$$

holds for all $u_e^{(k)} = (u^{(k)}, (u^{(k,\ell)})_{\ell \in \mathcal{N}_\Gamma^{(k)}}) \in V_e^{(k)}$.

Proof. Using the triangle inequality, we obtain

$$|u^{(k,\ell)}|_{L_\infty^0(\Gamma^{(k,\ell)})}^2 \lesssim |u^{(k)}|_{L_\infty^0(\Gamma^{(k,\ell)})}^2 + |u^{(k)} - u^{(k,\ell)}|_{L_\infty^0(\Gamma^{(k,\ell)})}^2.$$

As a next step, we apply Lemma 4.5 to the difference $|u^{(k)} - u^{(k,\ell)}|_{L_\infty^0(\Gamma^{(k,\ell)})}^2$. Since the L_∞ -norm does not change if we are on the physical or the parameter domain, we can apply Lemma 4.5 and subsequently utilize the equivalence of the norms on the parameter and the physical domain, cf. [29, Lemma 4.13] to get

$$|u^{(k)} - u^{(k,\ell)}|_{L_\infty^0(\Gamma^{(k,\ell)})}^2 \lesssim \|u^{(k)} - u^{(k,\ell)}\|_{L_2(\Gamma^{(k,\ell)})} \|u^{(k)} - u^{(k,\ell)}\|_{H^1(\Gamma^{(k,\ell)})}.$$

The triangle inequality allows to estimate

$$|u^{(k)} - u^{(k,\ell)}|_{L_\infty^0(\Gamma^{(k,\ell)})}^2 \lesssim \|u^{(k)} - u^{(k,\ell)}\|_{L_2(\Gamma^{(k,\ell)})} (\|u^{(k)} - c\|_{H^1(\Gamma^{(k,\ell)})} + \|u^{(k,\ell)} - c\|_{H^1(\Gamma^{(k,\ell)})})$$

for all $c \in \mathbb{R}$. The equivalence of the norms on the physical domain and the parameter domain, cf. [29, Lemma 4.13] and an inverse estimate, cf. [29, Lemma 4.3], give

$$\begin{aligned} &|u^{(k)} - u^{(k,\ell)}|_{L_\infty^0(\Gamma^{(k,\ell)})}^2 \\ &\lesssim \frac{p}{h_{k\ell}^{1/2}} \|u^{(k)} - u^{(k,\ell)}\|_{L_2(\Gamma^{(k,\ell)})} (\|u^{(k)} - c\|_{H^{1/2}(\Gamma^{(k,\ell)})} + \|u^{(k,\ell)} - c\|_{H^{1/2}(\Gamma^{(k,\ell)})}). \end{aligned}$$

We use $ab \lesssim a^2 + b^2$ and $(a + b)^2 \lesssim a^2 + b^2$ to get

$$\begin{aligned} &|u^{(k)} - u^{(k,\ell)}|_{L_\infty^0(\Gamma^{(k,\ell)})}^2 \\ &\lesssim \frac{p^2}{h_{k\ell}} \|u^{(k)} - u^{(k,\ell)}\|_{L_2(\Gamma^{(k,\ell)})}^2 + \|u^{(k)} - c\|_{H^{1/2}(\Gamma^{(k,\ell)})}^2 + \|u^{(k,\ell)} - c\|_{H^{1/2}(\Gamma^{(k,\ell)})}^2. \end{aligned}$$

Since this holds for all $c \in \mathbb{R}$, the Poincaré inequality gives further

$$|u^{(k)} - u^{(k,\ell)}|_{L_\infty^0(\Gamma^{(k,\ell)})}^2 \lesssim \frac{p^2}{h_{k\ell}} \|u^{(k)} - u^{(k,\ell)}\|_{L_2(\Gamma^{(k,\ell)})}^2 + |u^{(k)}|_{H^{1/2}(\Gamma^{(k,\ell)})}^2 + |u^{(k,\ell)}|_{H^{1/2}(\Gamma^{(k,\ell)})}^2.$$

Lemma 4.4 yields the final result. \square

[29, Lemma 4.17] states that the term $\Delta^{(k,\ell,i)}$ can be estimated by expressions which only involve patches sharing an edge. Now we prove a variant of [29, Lemma 4.18] that fits our needs.

Lemma 4.7. *For any two patches $\Omega^{(k)}$ and $\Omega^{(\ell)}$, sharing an edge $\Gamma^{(k,\ell)}$ which connects the vertices $\mathbf{x}^{(k,\ell,1)}$ and $\mathbf{x}^{(k,\ell,2)}$ and $\int_{\Gamma^{(k,\ell)}} u^{(k)}(s) - u^{(\ell,k)}(s) \, ds = 0$ and $i = 1, 2$, we have*

$$\Delta^{(k,\ell,i)} \lesssim \Lambda \left(|\mathcal{H}_h^{(k)} u^{(k)}|_{H^1(\Omega^{(k)})}^2 + |\mathcal{H}_h^{(\ell)} u^{(\ell)}|_{H^1(\Omega^{(\ell)})}^2 \right) + \frac{p^2}{h_{k\ell}} \|u^{(\ell)} - u^{(\ell,k)}\|_{L_2(\Gamma^{(k,\ell)})}^2$$

for all $u = (u_e^{(1)}, \dots, u_e^{(K)}) \in \widetilde{W}$, where $\Lambda = 1 + \log p + \max_{j=1,\dots,K} \log \frac{H_j}{h_j}$ and $\Delta^{(k,\ell,i)}$ is as in (26).

Proof. By the triangle inequality we have

$$\begin{aligned} \Delta^{(k,\ell,i)} &= |u^{(k)}(\mathbf{x}^{(k,\ell,i)}) - u^{(\ell,k)}(\mathbf{x}^{(k,\ell,i)})|^2 \\ &\lesssim |u^{(k)}(\mathbf{x}^{(k,\ell,i)}) - u^{(\ell)}(\mathbf{x}^{(k,\ell,i)})|^2 + |u^{(\ell)}(\mathbf{x}^{(k,\ell,i)}) - u^{(\ell,k)}(\mathbf{x}^{(k,\ell,i)})|^2. \end{aligned} \quad (27)$$

Let

$$\rho := \frac{1}{|\Gamma^{(k,\ell)}|} \left(\int_{\Gamma^{(k,\ell)}} u^{(k)} \, ds - \int_{\Gamma^{(k,\ell)}} u^{(\ell)} \, ds \right) = \frac{1}{|\Gamma^{(k,\ell)}|} \left(\int_{\Gamma^{(k,\ell)}} u^{(\ell,k)} \, ds - \int_{\Gamma^{(k,\ell)}} u^{(\ell)} \, ds \right)$$

and observe that the Cauchy-Schwarz inequality yields

$$\rho^2 \leq \frac{1}{|\Gamma^{(k,\ell)}|} \|u^{(\ell,k)} - u^{(\ell)}\|_{L_2(\Gamma^{(k,\ell)})}^2.$$

We further observe that due to Assumption 1, $|\Gamma^{(k,\ell)}| \approx \min\{H_k, H_\ell\}$. The triangle inequality yields

$$|u^{(k)}(\mathbf{x}^{(k,\ell,i)}) - u^{(\ell)}(\mathbf{x}^{(k,\ell,i)})|^2 \lesssim |(u^{(k)} - \rho)(\mathbf{x}^{(k,\ell,i)}) - u^{(\ell)}(\mathbf{x}^{(k,\ell,i)})|^2 + |\rho|^2.$$

Using [29, Lemma 4.18], we obtain further

$$\begin{aligned} &|u^{(k)}(\mathbf{x}^{(k,\ell,i)}) - u^{(\ell)}(\mathbf{x}^{(k,\ell,i)})|^2 \\ &\lesssim \Lambda (|\mathcal{H}_h^{(k)} u^{(k)}|_{H^1(\Omega^{(k)})}^2 + |\mathcal{H}_h^{(\ell)} u^{(\ell)}|_{H^1(\Omega^{(\ell)})}^2) + \frac{1}{\min\{H_k, H_\ell\}} \|u^{(\ell,k)} - u^{(\ell)}\|_{L_2(\Gamma^{(k,\ell)})}^2 \\ &\leq \Lambda (|\mathcal{H}_h^{(k)} u^{(k)}|_{H^1(\Omega^{(k)})}^2 + |\mathcal{H}_h^{(\ell)} u^{(\ell)}|_{H^1(\Omega^{(\ell)})}^2) + \frac{p^2}{h_{k\ell}} \|u^{(\ell,k)} - u^{(\ell)}\|_{L_2(\Gamma^{(k,\ell)})}^2. \end{aligned} \quad (28)$$

Now, we estimate $|u^{(\ell)}(\mathbf{x}^{(k,\ell,i)}) - u^{(\ell,k)}(\mathbf{x}^{(k,\ell,i)})|^2$ from above. To do so, we set $\widehat{u}^{(\ell)} = u^{(\ell)} \circ G_\ell$ and $\widehat{u}^{(\ell,k)} = u^{(\ell,k)} \circ G_k$. With unitary transformations, i.e., rotations and reflections, we can transform the patches such that the pre-image of $\Gamma^{(k,\ell)}$ is $(0, 1) \times \{0\}$ and that the pre-image of $\mathbf{x}^{(k,\ell,i)}$ is 0.

Let $\widetilde{u}^{(\ell)} := \widehat{u}^{(\ell)}(\cdot, 0)$ and $\widetilde{u}^{(\ell,k)} := \widehat{u}^{(\ell,k)}(\cdot, 0)$. Let η be the largest value such that $\widetilde{u}^{(\ell)}$ and $\widetilde{u}^{(\ell,k)}$ are polynomial on $(0, \eta)$. Using the quasi-uniformity assumption, cf. Assumption 4, we obtain $\eta \approx \widehat{h}_{k\ell}$. Arguments that are analogous to those used in the proof of Lemma 4.5, together with the inverse inequality [32, Theorem 4.76, eq. (4.6.5)] yield

$$\begin{aligned} |\widehat{u}^{(\ell)}(0) - \widehat{u}^{(\ell,k)}(0)|^2 &\lesssim \frac{1}{\eta} \|\widetilde{u}^{(\ell)} - \widetilde{u}^{(\ell,k)}\|_{L_2(0,\eta)}^2 + 2\|\widetilde{u}^{(\ell)} - \widetilde{u}^{(\ell,k)}\|_{L_2(0,\eta)} |\widetilde{u}^{(\ell)} - \widetilde{u}^{(\ell,k)}|_{H^1(0,\eta)} \\ &\lesssim \frac{1}{\eta} \|\widetilde{u}^{(\ell)} - \widetilde{u}^{(\ell,k)}\|_{L_2(0,\eta)}^2 + \frac{p^2}{\eta} \|\widetilde{u}^{(\ell)} - \widetilde{u}^{(\ell,k)}\|_{L_2(0,\eta)}^2. \end{aligned}$$

Since the L_2 -norm on $(0, 1)$ is larger than the L_2 -norm on $(0, \eta)$ and $\eta \approx \widehat{h}_{k\ell}$ we arrive at the estimate

$$|\widehat{u}^{(\ell)}(0) - \widehat{u}^{(\ell,k)}(0)|^2 \lesssim \frac{p^2}{\widehat{h}_{k\ell}} \|\widetilde{u}^{(\ell)} - \widetilde{u}^{(\ell,k)}\|_{L_2(0,1)}^2 = \frac{p^2}{\widehat{h}_{k\ell}} \|\widehat{u}^{(\ell)} - \widehat{u}^{(\ell,k)}\|_{L_2(\widehat{\Gamma}^{(k,\ell)})}^2.$$

An application of [29, Lemma 4.13] finally yields

$$|u^{(\ell)}(\mathbf{x}^{(k,\ell,i)}) - u^{(\ell,k)}(\mathbf{x}^{(k,\ell,i)})|^2 \lesssim \frac{p^2}{h_{k\ell}} \|u^{(\ell)} - u^{(\ell,k)}\|_{L_2(\Gamma^{(k,\ell)})}^2. \quad (29)$$

The combination of (27), (28) and (29) finishes the proof. \square

Before we give a proof of the main theorem, we estimate the sum of $w_\varepsilon^{(k)}$ -seminorms over all patches.

Lemma 4.8. *Let u and w be as in Lemma 4.3. Then, we have*

$$\begin{aligned} &\sum_{k=1}^K \sum_{\ell \in \mathcal{N}_\Gamma(k)} \left(|w^{(k)}|_{H^{1/2}(\Gamma^{(k,\ell)})}^2 + |w^{(k)}|_{L_\infty^0(\Gamma^{(k,\ell)})}^2 \right) \\ &\lesssim \sum_{k=1}^K \sum_{\ell \in \mathcal{N}_\Gamma(k)} \left(|u^{(k)}|_{H^{1/2}(\Gamma^{(k,\ell)})}^2 + |u^{(k)}|_{L_\infty^0(\Gamma^{(k,\ell)})}^2 + \frac{p^2}{h_{k\ell}} \|u^{(k,\ell)} - u^{(k)}\|_{L_2(\Gamma^{(k,\ell)})}^2 \right) \\ &\quad + \Lambda \sum_{k=1}^K |\mathcal{H}_h^{(k)} u^{(k)}|_{H^1(\Omega^{(k)})}^2, \end{aligned}$$

where $\Lambda := 1 + \log p + \max_{k=1,\dots,K} \log \frac{H_k}{h_k}$.

Proof. Lemma 4.3 yields

$$\begin{aligned} & \sum_{k=1}^K \sum_{\ell \in \mathcal{N}_\Gamma(k)} \left(|w^{(k)}|_{H^{1/2}(\Gamma^{(k,\ell)})}^2 + |w^{(k)}|_{L_\infty^0(\Gamma^{(k,\ell)})}^2 \right) \\ & \lesssim \sum_{k=1}^K \sum_{\ell \in \mathcal{N}_\Gamma(k)} \left(|u^{(k)}|_{H^{1/2}(\Gamma^{(k,\ell)})}^2 + |u^{(\ell,k)}|_{H^{1/2}(\Gamma^{(k,\ell)})}^2 + |u^{(k)}|_{L_\infty^0(\Gamma^{(k,\ell)})}^2 + |u^{(\ell,k)}|_{L_\infty^0(\Gamma^{(k,\ell)})}^2 \right) \\ & \quad + \sum_{k=1}^K \sum_{\ell \in \mathcal{N}_\Gamma(k)} \sum_{i=1}^2 \Delta^{(k,\ell,i)}. \end{aligned}$$

The Lemmas 4.4 and 4.6 and the observation $\ell \in \mathcal{N}_\Gamma(k) \Leftrightarrow k \in \mathcal{N}_\Gamma(\ell)$ yield further

$$\begin{aligned} & \sum_{k=1}^K \sum_{\ell \in \mathcal{N}_\Gamma(k)} \left(|w^{(k)}|_{H^{1/2}(\Gamma^{(k,\ell)})}^2 + |w^{(k)}|_{L_\infty^0(\Gamma^{(k,\ell)})}^2 \right) \\ & \lesssim \sum_{k=1}^K \sum_{\ell \in \mathcal{N}_\Gamma(k)} \left(|u^{(k)}|_{H^{1/2}(\Gamma^{(k,\ell)})}^2 + |u^{(k)}|_{L_\infty^0(\Gamma^{(k,\ell)})}^2 + \frac{p^2}{h_{k\ell}} \|u^{(\ell,k)} - u^{(\ell)}\|_{L_2(\Gamma^{(k,\ell)})}^2 \right) \\ & \quad + \sum_{k=1}^K \sum_{\ell \in \mathcal{N}_\Gamma(k)} \sum_{i=1}^2 \Delta^{(k,\ell,i)}. \end{aligned}$$

This finishes the proof for Alg. A and C, since $\Delta^{(k,\ell,i)} = 0$. For Alg. B, the desired result is a consequence of Lemma 4.7 and $|\mathcal{N}_\Gamma(k)| \leq 4$. \square

Lemma 4.9. *Let u and w be as in Lemma 4.3. Then, we have*

$$\begin{aligned} & \sum_{k=1}^K \sum_{\ell \in \mathcal{N}_\Gamma(k)} \frac{\delta p^2}{h_{k\ell}} \|w^{(k)} - w^{(k,\ell)}\|_{L_2(\Gamma^{(k,\ell)})}^2 \\ & \lesssim \Sigma \sum_{k=1}^K \sum_{\ell \in \mathcal{N}_\Gamma(k)} \left(\frac{\delta p^2}{h_{k\ell}} \|u^{(k)} - u^{(k,\ell)}\|_{L_2(\Gamma^{(k,\ell)})}^2 + \Lambda |\mathcal{H}_h^{(k)} u^{(k)}|_{H^1(\Omega^{(k)})}^2 \right), \end{aligned}$$

where

$$\Sigma := \begin{cases} 1 & \text{for Alg. A and C} \\ \delta p \max_{k=1,\dots,K} \max_{\ell \in \mathcal{N}_\Gamma(k)} \frac{h_k}{h_\ell} & \text{for Alg. B} \end{cases}. \quad (30)$$

Proof. We start with Alg. A and C. Lemma 4.3 and the observation that $\ell \in \mathcal{N}_\Gamma(k) \Leftrightarrow k \in \mathcal{N}_\Gamma(\ell)$ yield immediately

$$\begin{aligned} & \sum_{k=1}^K \sum_{\ell \in \mathcal{N}_\Gamma(k)} \frac{\delta p^2}{h_{k\ell}} \|w^{(k)} - w^{(k,\ell)}\|_{L_2(\Gamma^{(k,\ell)})}^2 \\ & \lesssim \sum_{k=1}^K \sum_{\ell \in \mathcal{N}_\Gamma(k)} \frac{\delta p^2}{h_{k\ell}} \left(\|u^{(k)} - u^{(k,\ell)}\|_{L_2(\Gamma^{(k,\ell)})}^2 + \sum_{i=1}^2 \frac{h_k}{p} \Delta^{(k,\ell,i)} \right). \end{aligned}$$

Since $\Delta^{(k,\ell,i)} = 0$ for Alg. A and C, this finishes the proof for this case. Now, consider the case of Alg. B. Lemma 4.7 and the observation that $\ell \in \mathcal{N}_\Gamma(k) \Leftrightarrow k \in \mathcal{N}_\Gamma(\ell)$ yield

$$\begin{aligned} & \sum_{k=1}^K \sum_{\ell \in \mathcal{N}_\Gamma(k)} \frac{\delta p^2}{h_{k\ell}} \|w^{(k)} - w^{(k,\ell)}\|_{L_2(\Gamma^{(k,\ell)})}^2 \\ & \lesssim \sum_{k=1}^K \sum_{\ell \in \mathcal{N}_\Gamma(k)} \frac{\delta p^2}{h_{k\ell}} \left(\|u^{(k)} - u^{(k,\ell)}\|_{L_2(\Gamma^{(k,\ell)})}^2 \right. \\ & \quad \left. + \Lambda \frac{h_k + h_\ell}{p} |\mathcal{H}_h^{(k)} u^{(k)}|_{H^1(\Omega^{(k)})}^2 + \frac{ph_k}{h_{k\ell}} \|u^{(\ell)} - u^{(\ell,k)}\|_{L_2(\Gamma^{(k,\ell)})}^2 \right). \end{aligned}$$

Using $h_{k\ell} = \min\{h_k, h_\ell\}$ and $\ell \in \mathcal{N}_\Gamma(k) \Leftrightarrow k \in \mathcal{N}_\Gamma(\ell)$, we immediately obtain the desired bound for Alg. B. \square

Now we are able to prove the bound for the condition number of the preconditioned dG IETI method as stated in Theorem 4.1.

Proof of Theorem 4.1. The idea of the proof is to use [23, Theorem 22], which states that

$$\kappa(M_{\text{sD}} F) \leq \sup_{\underline{u} \in \tilde{W}} \frac{\|B_D^\top B \underline{u}\|_S^2}{\|\underline{u}\|_S^2}, \quad (31)$$

where \underline{u} is the coefficient vector associated to the function $u = (u_e^{(1)}, \dots, u_e^{(K)}) = ((u^{(1)}, (u^{(1,\ell)})_{\ell \in \mathcal{N}_\Gamma(k)}, \dots))$. So, let u be arbitrary but fixed and let the function $w = (w_e^{(1)}, \dots, w_e^{(K)}) = ((w^{(1)}, (w^{(1,\ell)})_{\ell \in \mathcal{N}_\Gamma(k)}, \dots)$ with coefficient vector \underline{w} be such that $\underline{w} = B_D^\top B \underline{u}$. Moreover, let $v_e^{(k)} \in V_e^{(k)}$ be an arbitrary extension of $w_e^{(k)}$. Lemma 4.2 yields

$$\begin{aligned} \|B_D^\top B \underline{u}\|_S^2 &= \|\underline{w}\|_S^2 = \sum_{k=1}^K \|\mathcal{H}_A^{(k)} w_e^{(k)}\|_{a_e^{(k)}}^2 \\ &= \sum_{k=1}^K \inf_{w_0^{(k)} \in V_0^{(k)}} \|v_e^{(k)} - (w_0^{(k)}, 0^{|\mathcal{N}_\Gamma(k)|})\|_{a_e^{(k)}}^2 \approx \sum_{k=1}^K \inf_{w_0^{(k)} \in V_0^{(k)}} \|v_e^{(k)} - (w_0^{(k)}, 0^{|\mathcal{N}_\Gamma(k)|})\|_{d_e^{(k)}}^2 \\ &= \sum_{k=1}^K \inf_{w_0^{(k)} \in V_0^{(k)}} \left(|v^{(k)} - w_0^{(k)}|_{H^1(\Omega^{(k)})}^2 + \frac{\delta p^2}{h_{k\ell}} \sum_{\ell \in \mathcal{N}_\Gamma(k)} \|w^{(k)} - w^{(k,\ell)}\|_{L_2(\Gamma^{(k,\ell)})}^2 \right). \end{aligned}$$

Note that the second sum does not depend on $w_0^{(k)}$. Thus, the infimum refers only to the H^1 -seminorm, which means that that seminorm coincides with the seminorm of the (standard) discrete harmonic extension. Hence, we have

$$\|B_D^\top B \underline{u}\|_S^2 \approx \sum_{k=1}^K |\mathcal{H}_h^{(k)} w^{(k)}|_{H^1(\Omega^{(k)})}^2 + \sum_{k=1}^K \sum_{\ell \in \mathcal{N}_\Gamma(k)} \frac{\delta p^2}{h_{k\ell}} \|w^{(k)} - w^{(k,\ell)}\|_{L_2(\Gamma^{(k,\ell)})}^2. \quad (32)$$

First, we estimate the first sum in (32). [29, Theorem 4.2] yields

$$\sum_{k=1}^K |\mathcal{H}_h^{(k)} w^{(k)}|_{H^1(\Omega^{(k)})}^2 \lesssim p \sum_{k=1}^K |w^{(k)}|_{H^{1/2}(\partial\Omega^{(k)})}^2.$$

Using [29, Lemma 4.15], we get

$$\sum_{k=1}^K |\mathcal{H}_h^{(k)} w^{(k)}|_{H^1(\Omega^{(k)})}^2 \lesssim p \sum_{k=1}^K \sum_{\ell \in \mathcal{N}_\Gamma(k)} \left(|w^{(k)}|_{H^{1/2}(\Gamma^{(k,\ell)})}^2 + \Lambda |w^{(k)}|_{L^\infty(\Gamma^{(k,\ell)})}^2 \right).$$

Using $\Lambda \geq 1$ and Lemma 4.8, we obtain further

$$\begin{aligned} \sum_{k=1}^K |\mathcal{H}_h^{(k)} w^{(k)}|_{H^1(\Omega^{(k)})}^2 &\lesssim p\Lambda \sum_{k=1}^K \sum_{\ell \in \mathcal{N}_\Gamma(k)} \left(|u^{(k)}|_{H^{1/2}(\Gamma^{(k,\ell)})}^2 + |u^{(k)}|_{L^\infty(\Gamma^{(k,\ell)})}^2 \right) \\ &+ p\Lambda \sum_{k=1}^K \sum_{\ell \in \mathcal{N}_\Gamma(k)} \frac{p^2}{h_{k\ell}} \|u^{(k,\ell)} - u^{(k)}\|_{L_2(\Gamma^{(k,\ell)})}^2 + p\Lambda^2 \sum_{k=1}^K |\mathcal{H}_h^{(k)} u^{(k)}|_{H^1(\Omega^{(k)})}^2. \end{aligned}$$

Using [29, Lemma 4.15 and Theorem 4.2] and $|\mathcal{N}_\Gamma(k)| \leq 4$, we further estimate

$$\begin{aligned} \sum_{k=1}^K |\mathcal{H}_h^{(k)} w^{(k)}|_{H^1(\Omega^{(k)})}^2 &\lesssim p\Lambda^2 \sum_{k=1}^K |\mathcal{H}_h^{(k)} u^{(k)}|_{H^1(\Omega^{(k)})}^2 + p\Lambda \sum_{k=1}^K \sum_{\ell \in \mathcal{N}_\Gamma(k)} |u^{(k)}|_{L^\infty(\Gamma^{(k,\ell)})}^2 \\ &+ p\Lambda \sum_{k=1}^K \sum_{\ell \in \mathcal{N}_\Gamma(k)} \frac{p^2}{h_{k\ell}} \|u^{(k,\ell)} - u^{(k)}\|_{L_2(\Gamma^{(k,\ell)})}^2. \end{aligned}$$

Using [29, Lemma 4.14], we get further

$$\begin{aligned} \sum_{k=1}^K |\mathcal{H}_h^{(k)} w^{(k)}|_{H^1(\Omega^{(k)})}^2 &\lesssim p\Lambda^2 \sum_{k=1}^K |\mathcal{H}_h^{(k)} u^{(k)}|_{H^1(\Omega^{(k)})}^2 \\ &+ p\Lambda^2 \sum_{k=1}^K \sum_{\ell \in \mathcal{N}_\Gamma(k)} \left(|\mathcal{H}_h^{(k)} u^{(k)}|_{H^1(\Omega^{(k)})}^2 + (H_k)^{-2} \inf_{c \in \mathbb{R}} \|\mathcal{H}_h^{(k)} u^{(k)} - c\|_{L_2(\Omega^{(k)})}^2 \right) \\ &+ p\Lambda \sum_{k=1}^K \sum_{\ell \in \mathcal{N}_\Gamma(k)} \frac{p^2}{h_{k\ell}} \|u^{(k,\ell)} - u^{(k)}\|_{L_2(\Gamma^{(k,\ell)})}^2. \end{aligned}$$

$|\mathcal{N}_\Gamma(k)| \lesssim 1$ and the Poincaré inequality yield the estimate

$$\begin{aligned} &\sum_{k=1}^K |\mathcal{H}_h^{(k)} w^{(k)}|_{H^1(\Omega^{(k)})}^2 \\ &\lesssim p\Lambda^2 \sum_{k=1}^K \left(|\mathcal{H}_h^{(k)} u^{(k)}|_{H^1(\Omega^{(k)})}^2 + \sum_{\ell \in \mathcal{N}_\Gamma(k)} \frac{p^2}{h_{k\ell}} \|u^{(k,\ell)} - u^{(k)}\|_{L_2(\Gamma^{(k,\ell)})}^2 \right). \end{aligned} \tag{33}$$

To estimate the second sum in (32), we use Lemma 4.9 and obtain

$$\begin{aligned} & \sum_{k=1}^K \sum_{\ell \in \mathcal{N}_\Gamma(k)} \frac{\delta p^2}{h_{k\ell}} \|w^{(k)} - w^{(k,\ell)}\|_{L_2(\Gamma^{(k,\ell)})}^2 \\ & \lesssim \Sigma \sum_{k=1}^K \sum_{\ell \in \mathcal{N}_\Gamma(k)} \left(\frac{\delta p^2}{h_{k\ell}} \|u^{(k)} - u^{(k,\ell)}\|_{L_2(\Gamma^{(k,\ell)})}^2 + \Lambda |\mathcal{H}_h^{(k)} u^{(k)}|_{H^1(\Omega^{(k)})}^2 \right), \end{aligned} \quad (34)$$

where Σ is as in (30). The combination of $\delta \gtrsim 1$, $\Lambda \geq 1$, $\Sigma \geq 1$, (32), (33) and (34) yields

$$\begin{aligned} \|B_D^\top B \underline{u}\|_S^2 & \lesssim (p\Lambda^2 + \Sigma\Lambda) \sum_{k=1}^K \left(|\mathcal{H}_h^{(k)} u^{(k)}|_{H^1(\Omega^{(k)})}^2 + \sum_{\ell \in \mathcal{N}_\Gamma(k)} \frac{\delta p^2}{h_{k\ell}} \|u^{(k)} - u^{(k,\ell)}\|_{L_2(\Gamma^{(k,\ell)})}^2 \right) \\ & = (p\Lambda^2 + \Sigma\Lambda) \|u\|_d^2 \approx (p\Lambda^2 + \Sigma\Lambda) \|\underline{u}\|_S^2 \lesssim \Sigma\Lambda^2 \|\underline{u}\|_S^2. \end{aligned}$$

The combination of this estimate and (31) finishes the proof. \square

5 Numerical results

In this section, we present the results of our numerical experiments that illustrate the presented convergence theory. We consider the Poisson problem

$$\begin{aligned} -\Delta u(x, y) &= 2\pi^2 \sin(\pi x) \sin(\pi y) & \text{for } (x, y) \in \Omega \\ u &= 0 & \text{on } \partial\Omega, \end{aligned}$$

where the computational domain Ω is one of the domains depicted in Figure 4.

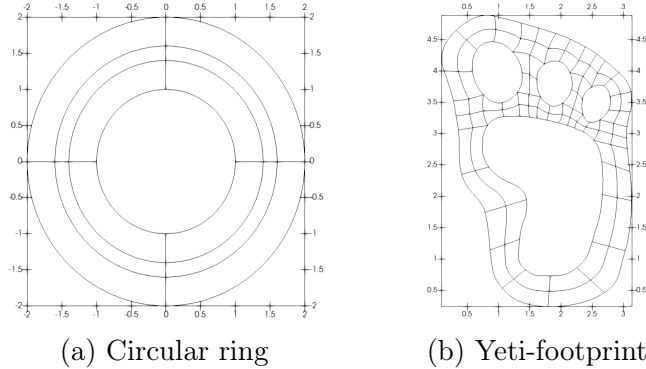


Figure 4: Computational domains and the decomposition into patches

The first domain (Figure 4a) is a circular ring consisting of 12 patches. Each of them is the image of a NURBS mapping of degree 2. The second domain (Figure 4b) is the

r \ p	2		3		4		5		6		7		8	
	it	κ	it	κ	it	κ	it	κ	it	κ	it	κ	it	κ
2	10	5.65	12	6.23	12	6.53	13	7.06	13	7.28	14	7.77	14	7.93
3	12	6.29	12	6.93	13	7.44	13	7.90	14	8.33	14	8.67	15	9.03
4	13	7.04	13	7.88	14	8.53	14	9.09	15	9.59	15	10.00	15	10.37
5	13	8.00	14	9.06	15	9.82	15	10.47	16	11.03	16	11.49	16	11.91
6	15	9.19	16	10.42	16	11.29	17	12.02	16	12.64	18	13.16	17	13.63
7	16	10.58	17	11.97	18	12.94	18	13.74	18	14.43	18	15.01	17	15.52
8	17	12.14	18	13.69	18	14.76	19	15.65	19	16.40	19	17.02	19	17.58

Table 1: Iteration counts (it) and condition numbers (κ); Alg. A; triple ring

r \ p	2		3		4		5		6		7		8	
	it	κ	it	κ	it	κ	it	κ	it	κ	it	κ	it	κ
2	36	275	43	348	50	414	49	472	52	547	52	618	56	727
3	38	294	44	361	48	433	50	521	52	571	54	678	55	739
4	44	311	49	396	49	452	51	544	52	605	55	700	55	764
5	48	342	47	401	50	477	51	567	53	649	55	723	57	830
6	50	357	50	425	52	510	54	585	55	681	56	759	58	866
7	49	379	52	461	55	554	57	628	58	708	60	811	62	903
8	53	404	53	474	56	577	59	677	59	753	64	878	65	978

Table 2: Iteration counts (it) and condition numbers (κ); Alg. B; triple ring

Yeti-footprint which is composed of 84 patches. In this case, all of the patches are parameterized using B-spline functions, again of degree 2.

The numerical experiments are carried out with B-spline discretization spaces of maximum smoothness on grids that are constructed as follows. For the circular ring, the coarsest grid on each patch only consists of one element, i.e., the discretization space (on the parameter domain) for each patch consists only of polynomial functions. For the Yeti-footprint, the coarsest grid for the 20 patches in the bottom of the domain consists of two elements per patch. The grid is constructed by adding an edge that connects the midpoints of the two longer sides of the patch. The other patches of the Yeti-footprint only consist of one element. For both domains, the finer grids are constructed by refinement. For the first refinement step, i.e., for $r = 1$, we insert one knot into each knot span. The new knot is not located in the center, but at $4/9$ times

r \ p	2		3		4		5		6		7		8	
	it	κ	it	κ	it	κ	it	κ	it	κ	it	κ	it	κ
2	7	1.60	10	2.25	10	2.45	11	2.55	11	2.80	12	2.89	12	3.13
3	10	2.28	10	2.56	11	2.81	11	3.04	11	3.24	12	3.43	12	3.58
4	11	2.62	11	3.03	12	3.35	11	3.63	12	3.88	13	4.08	13	4.27
5	11	3.09	12	3.62	12	4.00	13	4.32	13	4.59	14	4.81	14	5.01
6	12	3.69	13	4.30	14	4.72	14	5.07	14	5.36	15	5.61	15	5.82
7	13	4.37	14	5.04	15	5.50	15	5.88	16	6.20	16	6.46	16	6.69
8	14	5.13	15	5.86	16	6.35	16	6.75	17	7.09	17	7.37	17	7.61

Table 3: Iteration counts (it) and condition numbers (κ); Alg. C; triple ring

r \ p	2		3		4		5		6		7		8	
	it	κ	it	κ	it	κ	it	κ	it	κ	it	κ	it	κ
1	10	2.09	12	2.73	14	3.27	15	3.80	16	4.20	18	4.67	19	5.00
2	12	2.82	14	3.56	15	4.11	16	4.60	17	5.01	19	5.43	20	5.77
3	14	3.77	16	4.61	17	5.24	18	5.77	19	6.22	20	6.63	21	6.97
4	16	4.86	17	5.83	19	6.54	20	7.13	21	7.64	22	8.06	23	8.46
5	19	6.12	20	7.21	21	8.00	22	8.65	23	9.21	24	9.73	24	10.13
6	21	7.54	22	8.74	23	9.61	24	10.37	25	10.98	25	11.50	26	11.96
7	22	9.11	24	10.44	25	11.38	26	12.23	27	12.89	27	13.50	27	14.02

Table 4: Iteration counts (it) and condition numbers (κ); Alg. A; Yeti-footprint

the length of the knot span if the patch index k is even and at 6/11 times that length if k is odd. The subsequent refinement steps $r = 2, 3, \dots$ are done uniformly. This refinement procedure yields discretizations that are non-matching at the interfaces.

For these discretization spaces, we set up a dG IETI discretization as introduced in Section 3. To solve the system (21), we use a preconditioned conjugate gradient (PCG) method with the proposed scaled Dirichlet preconditioner M_{SD} . The implementation is done using G+Smo [24]. The local subproblems are solved with the sparse direct solver from the PARDISO project¹.

For all numerical experiments, we start the iteration with a randomly sampled vector with entries in the interval $[-1, 1]$. The stopping criterion is chosen as follows. The

¹<https://www.pardiso-project.org/>

r \ p	2		3		4		5		6		7		8	
	it	κ	it	κ	it	κ	it	κ	it	κ	it	κ	it	κ
1	42	27	49	39	57	52	65	68	72	80	82	97	90	117
2	44	33	50	45	56	58	61	74	69	88	75	103	84	122
3	49	41	54	56	59	70	64	87	70	100	76	119	81	132
4	53	51	60	65	63	84	69	97	74	119	80	132	85	156
5	59	57	64	75	70	90	75	112	80	135	84	149	90	171
6	62	66	68	83	74	101	79	127	85	147	89	170	96	191
7	65	75	74	97	79	117	83	146	88	164	94	188	100	215

Table 5: Iteration counts (it) and condition numbers (κ); Alg. B; Yeti-footprint

r \ p	2		3		4		5		6		7		8	
	it	κ	it	κ	it	κ	it	κ	it	κ	it	κ	it	κ
1	6	1.16	7	1.27	9	1.43	10	1.57	11	1.71	12	1.83	12	1.95
2	7	1.32	9	1.49	10	1.67	11	1.81	12	1.95	13	2.09	13	2.19
3	9	1.57	10	1.81	11	2.00	12	2.17	12	2.28	14	2.46	15	2.58
4	11	1.89	12	2.18	13	2.41	13	2.59	14	2.76	15	2.91	16	3.05
5	12	2.26	13	2.61	14	2.87	15	3.06	16	3.27	16	3.42	17	3.57
6	14	2.70	15	3.09	16	3.38	16	3.61	17	3.82	18	4.00	19	4.17
7	15	3.19	16	3.63	17	3.95	18	4.21	18	4.43	19	4.63	20	4.81

Table 6: Iteration counts (it) and condition numbers (κ); Alg. C; Yeti-footprint

iteration stops if the the l_2 -norm of the residual vector drops below 10^{-6} times the residual of the right-hand side. For each experiment, we show the number of iterations (it) required to reach the stopping criterion and an estimate of the condition number (κ) of the preconditioned system matrix $M_{sD}F$ that has been derived using the PCG algorithm.

We start with the numerical experiments for the circular ring (Figure 4a). Table 1 shows the results for Alg. A (vertex values). We observe in that the condition number grows not more than $\log^2 H/h$. Moreover, we also observe a weak growth in the spline degree, which is smaller than the linear growth predicted by the theory. Table 2 shows the results for Alg. B (edge averages). Here, the condition numbers are much larger than before. The dependence on the grid size and the spline degree seems to be the same as for Alg. A. The Table 3 comprises the data collected for Alg. C (vertex

e \ p	2		3		4		5		6		7		Alg.
	it	κ	it	κ	it	κ	it	κ	it	κ	it	κ	
1	14	8	14	9	15	9	16	10	16	10	16	11	} A
2	14	8	15	9	15	9	16	10	16	10	17	11	
3	14	8	15	9	15	9	16	10	17	10	18	11	
1	49	338	50	437	52	500	55	622	58	698	61	769	} B
2	52	486	55	603	59	743	65	893	67	1041	72	1196	
3	64	852	71	1072	75	1317	77	1619	80	1841	89	2122	

Table 7: Iteration counts (it) and condition numbers (κ) depending on grid size disparity; triple ring

e \ p	2		3		4		5		6		7		Alg.
	it	κ	it	κ	it	κ	it	κ	it	κ	it	κ	
1	15	5	17	5	18	6	19	7	19	7	21	7	} A
2	17	5	18	6	19	7	19	7	20	8	22	8	
3	17	6	19	7	19	8	20	8	21	9	22	9	
1	54	52	60	69	65	83	70	99	73	120	79	137	} B
2	62	72	69	96	76	123	78	151	84	177	90	215	
3	77	133	87	182	95	233	103	278	110	335	115	390	

Table 8: Iteration counts (it) and condition numbers (κ) depending on grid size disparity; Yeti-footprint

values + edge averages). As expected, this approach yields the smallest values for the condition numbers. The condition number seems to grow only like \sqrt{p} in the spline degree and like $\log H/h$ in the grid size.

Next, we will take a look at the results on the Yeti-footprint (Figure 4b). Table 4 reports on the results for Alg. A. We can again see that the increase in the condition number is like $\log^2 H/h$ and the increase in p is sub-linear, almost like \sqrt{p} . Table 5 gives the condition number estimates for Alg. B, where we observe that the condition number grows almost linearly in the spline degree p (which indicates that the convergence theory might be sharp in this respect). Alg. C, whose results are given in Table 6, yields again the best condition numbers. Compared to the circular ring, the condition numbers for the Yeti-footprint are smaller, which might be connected to a more regular geometry mapping.

Finally, we present an experiment that indicates that the dependence of the condition number on the ratio of the grid sizes of neighboring patches ($\max_{k=1,\dots,K} \max_{\ell \in \mathcal{N}_\Gamma(k)} \frac{h_k}{h_\ell}$) is only present for Alg. B. For this purpose, we compare Alg. A with Alg. B on both computational domains for particular grids that are constructed as follows. Starting from the initial grid introduced above, we applied 4 refinement steps as above. Then, we uniformly refine the grids on all patches $\Omega^{(k)}$, where k is even, additionally $e \in \{1, 2, 3\}$ times. Thus, the grid sizes between patches with even and odd degrees vary by a factor of 2^e . We observe in Table 7 for the circular ring and in Table 8 for the Yeti-footprint that the condition number is almost independent of e if Alg. A is used, while it increases like 2^e if Alg. B is chosen. This means that the condition number grows linearly in the ratio of the grid sizes, which coincides with the prediction of the convergence theory.

6 Conclusions

In this paper, we have extended the theory from [29], where we established p -explicit condition number estimates for continuous Galerkin IETI-DP solvers, to symmetric interior penalty discontinuous Galerkin discretizations. Again, we have analyzed both the dependence on the grid size and the spline degree. If the vertex values are chosen as primal degrees of freedom (Alg. A and C), the results are the same as for conforming discretizations. If we use only the edge averages (Alg. B), the condition number estimate additionally depends on the ratio between the grid sizes of neighboring patches. This can also be observed in the numerical experiments.

Alg. B does not perform as good as the other options. However, this approach seems to be beneficial if a non-conforming decomposition of the overall domain into patches is considered, like a decomposition with T-junctions. Although the IETI-DP methods also perform well on domains with non-trivial geometry functions, analyzing the dependence of the condition number on the geometry function is an interesting topic for future research.

Acknowledgments. The first author was supported by the Austrian Science Fund (FWF): S117 and W1214-04. Also, the second author has received support from the Austrian Science Fund (FWF): P31048. Finally, the authors want to thank Ulrich Langer for fruitful discussions and help with the study of existing literature.

References

- [1] R. Adams and J. Fournier. *Sobolev Spaces*. Elsevier Science, 2003.
- [2] M. Ainsworth. A Preconditioner Based on Domain Decomposition for h - p Finite-Element Approximation on Quasi-uniform Meshes. *SIAM J. Numer. Anal.*,

- 33(4):1358–1376, 1996.
- [3] P. Antonietti and P. Houston. A Class of Domain Decomposition Preconditioners for hp -Discontinuous Galerkin Finite Element Methods. *J. Sci. Comput.*, 46(1):124–149, 2011.
- [4] P. F. Antonietti and B. Ayuso. Schwarz domain decomposition preconditioners for discontinuous Galerkin approximations of elliptic problems: non-overlapping case. *ESAIM: Math. Model. Numer. Anal.*, 41(1):21–54, 2007.
- [5] D. Arnold. An interior penalty finite element method with discontinuous elements. *SIAM J. Numer. Anal.*, 19(4):742 – 760, 1982.
- [6] D. Arnold, F. Brezzi, B. Cockburn, and L. Marini. Unified analysis of discontinuous Galerkin methods for elliptic problems. *SIAM J. Numer. Anal.*, 39(5):1749 – 1779, 2002.
- [7] C. Canuto, L. Pavarino, and A. Pieri. BDDC preconditioners for continuous and discontinuous Galerkin methods using spectral/ hp elements with variable local polynomial degree. *IMA J. Numer. Anal.*, 34(3):879–903, 2014.
- [8] J. A. Cottrell, T. J. R. Hughes, and Y. Bazilevs. *Isogeometric Analysis – Toward Integration of CAD and FEA*. John Wiley & Sons, 2009.
- [9] L. Diosady and D. Darmofal. BDDC for Higher-Order Discontinuous Galerkin Discretizations. In R. Bank, M. Holst, O. Widlund, and J. Xu, editors, *Domain Decomposition Methods in Science and Engineering XX*, pages 559–567. Springer Berlin Heidelberg, 2013.
- [10] M. Dryja, J. Galvis, and M. Sarkis. BDDC methods for discontinuous Galerkin discretization of elliptic problems. *J. Complex.*, 23(4):715–739, 2007.
- [11] M. Dryja, J. Galvis, and M. Sarkis. A FETI-DP Preconditioner for a Composite Finite Element and Discontinuous Galerkin Method. *SIAM J. Numer. Anal.*, 51(1):400–422, 2013.
- [12] C. Farhat and F.-X. Roux. A Method of Finite Element Tearing and Interconnecting and its Parallel Solution Algorithm. *Int. J. Numer. Methods Eng.*, 32(6):1205–1227, 1991.
- [13] B. Guo and W. Cao. Additive Schwarz Methods for the h - p Version of the Finite Element Method in Two Dimensions. *SIAM J. Sci. Comput.*, 18(5):1267–1288, 1997.
- [14] C. Hofer. Analysis of discontinuous Galerkin dual-primal isogeometric tearing and interconnecting methods. *Math. Models Methods Appl. Sci.*, 28(1):131–158, 2018.

- [15] C. Hofer and U. Langer. Dual-primal isogeometric tearing and interconnecting solvers for multipatch continuous and discontinuous Galerkin IgA equations. *PAMM*, 16(1):747–748, 2016.
- [16] C. Hofer and U. Langer. Dual-Primal Isogeometric Tearing and Interconnecting Methods. In B. N. Chetverushkin, W. Fitzgibbon, Y. Kuznetsov, P. Neittaanmäki, J. Periaux, and O. Pironneau, editors, *Contributions to Partial Differential Equations and Applications*, pages 273–296. Springer International Publishing, 2019.
- [17] T. J. R. Hughes, J. A. Cottrell, and Y. Bazilevs. Isogeometric analysis: CAD, finite elements, NURBS, exact geometry and mesh refinement. *Comput. Methods Appl. Mech. Eng.*, 194(39-41):4135 – 4195, 2005.
- [18] A. Klawonn, L. Pavarino, and O. Rheinbach. Spectral element FETI-DP and BDDC preconditioners with multielement subdomains. *Comput. Methods Appl. Mech. Eng.*, 198(3-4):511 – 523, 2008.
- [19] S. Kleiss, C. Pechstein, B. Jüttler, and S. Tomar. IETI-Isogeometric Tearing and Interconnecting. *Comput. Methods Appl. Mech. Eng.*, 247-248:201–215, 2012.
- [20] V. G. Korneev and U. Langer. *Dirichlet–Dirichlet Domain Decomposition Methods for Elliptic Problems*. World Scientific, 2015.
- [21] U. Langer, A. Mantzaflaris, S. E. Moore, and I. Touloupoulos. Multipatch Discontinuous Galerkin Isogeometric Analysis. In B. Jüttler and B. Simeon, editors, *Isogeometric Analysis and Applications 2014*, pages 1–32. Springer International Publishing, 2015.
- [22] U. Langer and I. Touloupoulos. Analysis of multipatch discontinuous Galerkin IgA approximations to elliptic boundary value problems. *Comp. Vis. Sci.*, 17(5):217 – 233, 2015.
- [23] J. Mandel, C. R. Dohrmann, and R. Tezaur. An algebraic theory for primal and dual substructuring methods by constraints. *Appl. Numer. Math.*, 54(2):167–193, 2005.
- [24] A. Mantzaflaris, R. Schneckleitner, S. Takacs, and others (see website). G+Smo (Geometry plus Simulation modules). <http://github.com/gismo>, 2020.
- [25] L. F. Pavarino. BDDC and FETI-DP preconditioners for spectral element discretizations. *Comput. Methods Appl. Mech. Eng.*, 196(8):1380 – 1388, 2007.
- [26] L. F. Pavarino and O. B. Widlund. A Polylogarithmic Bound for an Iterative Substructuring Method for Spectral Elements in Three Dimensions. *SIAM J. Numer. Anal.*, 33(4):1303 – 1335, 1996.

- [27] C. Pechstein. *Finite and Boundary Element Tearing and Interconnecting Solvers for Multiscale Problems*. Springer, Heidelberg, 2013.
- [28] B. Rivière. *Discontinuous Galerkin Methods for Solving Elliptic and Parabolic Equations*. Society for Industrial and Applied Mathematics, 2008.
- [29] R. Schneckleitner and S. Takacs. Condition number bounds for IETI-DP methods that are explicit in h and p , 2019. Submitted. <https://arxiv.org/pdf/1912.07909.pdf>.
- [30] J. Schöberl and C. Lehrenfeld. Domain Decomposition Preconditioning for High Order Hybrid Discontinuous Galerkin Methods on Tetrahedral Meshes. In T. Apel and O. Steinbach, editors, *Advanced Finite Element Methods and Applications*, volume 66, pages 27–56. Springer Berlin Heidelberg, 2013.
- [31] J. Schöberl, J. Melenk, C. Pechstein, and S. Zaglmayr. Schwarz preconditioning for high order simplicial finite elements. In O. B. Widlund and D. E. Keyes, editors, *Domain Decomposition Methods in Science and Engineering XVI*, pages 139–150. Springer Berlin Heidelberg, 2007.
- [32] C. Schwab. *p - and hp - Finite Element Methods: Theory and Applications in Solid and Fluid Mechanics*. Clarendon Press, 1998.
- [33] S. Takacs. A quasi-robust discretization error estimate for discontinuous Galerkin Isogeometric Analysis, 2019. Submitted. <https://arxiv.org/pdf/1901.03263.pdf>.
- [34] A. Toselli and O. B. Widlund. *Domain Decomposition Methods – Algorithms and Theory*. Springer, Berlin, 2005.